



<https://technobius.kz/>

e-ISSN  
2789-7338

# Technobius

*A peer-reviewed open-access journal*

*Technobius, LLP*

*Volume 4, No. 1, 2024*



# Technobius

Volume 4, No. 1, 2024



A peer-reviewed open-access journal registered by the Ministry of Information and Social Development of the Republic of Kazakhstan, Certificate № KZ00VPY00039799 dated 7.09.2021

**ISSN (Online):** 2789-7338

**Thematic Directions:** Construction and Materials Science




**Publisher:** Technobius, LLP

**Address:** 17A Momyshuly street, office 22, 010000, Astana, Republic of Kazakhstan




**Editor-in-Chief:**

   *Yelbek Utepov*, PhD, Professor, Department of Civil Engineering, L.N. Gumilyov Eurasian National University, Astana, Kazakhstan




**Technical Editor:**




   *Assel Tulebekova*, PhD, Professor, Department of Civil Engineering, L.N. Gumilyov Eurasian National University, Astana, Kazakhstan

**Editors:**




   *Yuri Pukhareenko*, Doctor of Technical Sciences, Professor, Department of Building Materials Technology and Metrology, Saint Petersburg State University of Architecture and Civil Engineering, Saint Petersburg, Russian Federation




   *Askar Zhussupbekov*, Doctor of Technical Sciences, Professor, Department of Civil Engineering, L.N. Gumilyov Eurasian National University, Astana, Kazakhstan




   *Evgeniya Tkach*, Doctor of Technical Sciences, Professor, Department of Building Materials Science, Moscow State University of Civil Engineering, Moscow, Russian Federation




   *Ignacio Menéndez Pidal de Navascués*, Doctor of Technical Sciences, Professor, Department of Civil Engineering, Technical University of Madrid, Madrid, Spain




   *Irina Aubakirova*, Candidate of Technical Sciences, Associate Professor, Department of Building Materials Technology and Metrology, Saint Petersburg State University of Architecture and Civil Engineering, Saint Petersburg, Russian Federation




   *Zeljko Kos*, PhD, Assistant Professor, Department of Civil Engineering, University North, Varaždin, Croatia

   *Aleksej Aniskin*, Candidate of Technical Sciences, Assistant Professor, Department of Civil Engineering, University North, Varaždin, Croatia

   *Daniyar Akhmetov*, Doctor of Technical Sciences, Associate Professor, Department of Construction and Building materials, Satbayev University, Almaty, Kazakhstan

   *Zhanbolat Shakhmov*, PhD, Associate Professor, Department of Civil Engineering, L.N. Gumilyov Eurasian National University, Astana, Kazakhstan

   *Timoth Mkilima*, PhD, Lecturer, Department of Environmental Engineering and Management, the University of Dodoma, Dodoma, Tanzania

   *Aliya Aldungarova*, PhD, Associate Professor, School of Architecture, Civil Engineering and Energy, D. Serikbayev East Kazakhstan technical university, Ust-Kamenogorsk, Kazakhstan

**Copyright:** © Technobius, LLP

**Contacts:** Website: <https://technobius.kz/>  
E-mail: [technobius.research@gmail.com](mailto:technobius.research@gmail.com)

**CONTENTS**

<b>Title and Authors</b>	<b>Category</b>	<b>No.</b>
Assessment of mechanical properties of elements modular block <i>Ulan Altigenov, Aliy Bespaev, Natalya Ryvkina, Ilya Teshev</i>	<i>Construction</i>	0051
Research of foam concrete quality by two-stage foam injection method in comparison with classical foam concrete <i>Rauan Lukpanov, Duman Dyusseminov, Aliya Altynbekova, Zhibek Zhantlesova, Tattigul Seidmarova</i>	<i>Materials Science</i>	0052
Geotechnical interpolation methodology for determining intermediate values of soil properties <i>Aliya Aldungarova, Assel Mukhamejanova, Nurgul Alibekova, Sabit Karaulov, Daniyar Akhmetov</i>	<i>Construction</i>	0053
Calculation and numerical modeling of the effect of heat and mass transfer on the properties of pile foundations in seasonally freezing soils <i>Saltanat Mussakhanova, Assel Sarsembayeva, Askar Zhussupbekov, Philip Collins</i>	<i>Construction</i>	0054
Comparative study of pile quality control techniques <i>Abdulla Omarov, Yoshinori Iwasaki</i>	<i>Construction</i>	0055



## Assessment of mechanical properties of elements modular block

Ulan Altigenov<sup>1,\*</sup>, Aliy Bespaev<sup>2</sup>, Natalya Ryvkina<sup>1</sup>, Ilya Teshev<sup>3</sup>

<sup>1</sup>Department of Civil Engineering, L.N. Gumilyov Eurasian National University, Astana, Kazakhstan

<sup>2</sup>Kazakh Scientific Research and Design Institute of Civil Engineering and Architecture, JSC, Almaty, Kazakhstan

<sup>3</sup>Department of Civil Engineering, Satbayev University, Almaty, Kazakhstan

\*Correspondence: [860806301721@enu.kz](mailto:860806301721@enu.kz)

**Abstract.** This study presents the control test process to assess the bearing capacity, crack resistance, and crack opening width of the volume block ceiling slabs and the floor slab of the inter-block corridor. These parameters play an important role in ensuring the reliability and durability of buildings, especially when volumetric blocks are used in construction. The study's first phase focuses on the methodology of load-carrying capacity testing of ceiling slabs. The study's second phase focuses on the materials' crack resistance. The analysis of cracks in the material structure is a key aspect since cracks can lead to deterioration of its mechanical properties and reduced durability. The third stage of the study focuses on the crack opening width. This parameter is important in determining the criticality of cracks and their effect on structural integrity. The fourth stage of the study covers the analysis of the floor slabs of the interlocking corridor. Considering the peculiarities of loads and operating conditions in this context, tests analyzing the bearing capacity and stability of the slabs are carried out. The crack opening width reached 0.9 mm and the vertical deflections exceeded 50 mm, the deflection in the inter-block corridor floor slab before failure was about 11 mm. The test results indicate its sufficient strength, stiffness, and crack resistance. The study provides a deeper understanding of the properties and characteristics of materials used in construction and optimizes their use to improve the strength and durability of buildings.

**Keywords:** volume blocks, crack resistance, stiffness, strength, load, assessment.

### 1. Introduction

The current stage of development of large cities is marked by a significant change in the structure towards the introduction of innovative structural solutions based on the use of multi-story buildings made of prefabricated reinforced concrete structures. This is explained by the desire for modern and efficient construction methods necessary to meet the growing needs of urbanization [1]. The resurgence of high-rise residential building construction using volumetric blocks represents a significant transition in the construction industry. This approach involves the assembly of pre-designed and prefabricated modules directly at the construction site, which provides a more systematic and efficient construction process. The modular construction method offers several advantages such as shorter project time, reduced construction cost, and increased flexibility in design [2]. In addition, it complies with the principles of sustainable construction by minimizing waste and optimizing the use of resources.

Prefabricated modules provide more precise control over the materials used, which contributes to more efficient use of resources. In addition, the controlled environment in which these modules are manufactured reduces the overall environmental footprint of the construction work. With a growing population and increasing environmental concerns, modular construction acts as a sustainable solution to address these issues. The materials used in modern modular construction also contribute to the structural integrity and sustainability of buildings [3].

One of the key areas of technical advancement in the use of volumetric blocks also lies in design methodology [4]. Traditional construction often adheres to linear and sequential design

processes, whereas modular construction allows for a more integrated and parallel approach. Studies have noted a shift towards the use of modern computer-aided design (CAD) software and building information modeling (BIM) tools to facilitate the design of modular components [5]. The ability to visualize and model modular structures in a digital environment allows architects and engineers to optimize designs in terms of efficiency, aesthetics, and functionality.

In practice, the system of construction with the use of volume blocks is extensive. Thus, in the construction of residential and civil buildings "Variel" (Elkon, Switzerland) uses volume blocks of open type, assembled from two load-bearing end panels or portal reinforced concrete frames, prestressed ribbed floor panels, and ceiling slab [6]. The average factory availability of volumetric blocks is 70-80%.

In Sweden, the firm "Boštodsbolaget" (Gothenburg) builds houses with 10 floors of the height of panel-block system from blocks of "glass" type of various typo-sizes [7]. The bearing walls of the blocks are 7-16 cm thick and made of concrete of 250 grade. I

n Finland, the system of volume-block housebuilding "Ausa" is developed, in which ribbed volume blocks of the "pipe" type are made in the size for the width of the building with the linear transmission of vertical loads on the long sides.

In Brasov (Romania) the experimental construction of about 200 buildings up to 5 stories high from volume blocks of the "cap" type has been carried out. From the international experience of construction of buildings from volumetric blocks, we can note the construction of low-rise buildings in Belgium, Sweden, Peru, and Dubai, as well as high-rise buildings in New York and Singapore.

From the modern European experience, it should be noted the construction of low-rise buildings with full factory finishing in Germany [8]. The modern stage of development of large cities of the Republic of Kazakhstan also applies structural solutions of multi-story buildings from prefabricated reinforced concrete structures [9]. In this regard, this study is related to the study of the operation of volumetric blocks at all stages of loading by vertical load, control tests.

## 2. Methods

The paper considers the control tests to check the bearing capacity, crack resistance, and crack opening width in the ceiling slabs of the volume blocks; and in the floor slab of the inter-unit corridor [10]. The strength, stiffness, and crack resistance of the floor and ceiling slabs of the volume blocks, as well as the floor slab of the inter-unit corridor, are evaluated by testing these elements under the action of uniformly distributed vertical load [11].

Claydite concrete blocks are made of the "lying glass" type with dimensions of 3480x6980x2980 mm, consisting of three walls, ceiling, and floor slabs. The volumetric modules are completed with prefabricated load-bearing exterior wall panels. According to the structural solution of buildings from volume, modules are volume-block buildings with internal single-layer walls and inserted external walls of both single-layer and three-layer execution [12].

The building is made of volume blocks supported on each other, with linear support on four sides through a layer of mortar. The volume blocks are connected horizontally by welding plates located on the ceiling.

Horizontal loads are taken by connecting elements located on three sides of the volume block. Volumetric blocks have two side walls of ribbed design with a wall thickness of 50 mm and rib height of 100 mm, as well as an end flat wall thickness of 100 mm.

The floor slab of the volume block is ribbed with a shelf 80 mm thick and ribs 170 mm high. The ceiling slab of the volume block is flat with a runaway 80-97 mm thick. Volumetric blocks are reinforced with spatial frames and reinforcement meshes united in a single spatial block (Figure 1).

The externally inserted wall panels with a total thickness of 120 mm are single-layer with a load-bearing layer of expanded clay, effective insulation, and a cladding layer in the form of a curtain wall system. The ceiling slab also integrates the walls of the volume block into a single system and is loaded vertically only by the slab's mass.





Figure 1 – Test bench with volumetric block

The volume block used for these tests with dimensions 6980x3480x2980 mm is made of expanded clay concrete of strength class LC 20/22 (B20) density class  $\rho = 800 \text{ kg/m}^3$ . The ceiling slab is a flat reinforced concrete slab of variable thickness with a slope from 97 mm to 80 mm. The ceiling slab is reinforced with a lower mesh of  $\text{Ø}4 \text{ S400C (Vr400)}$  reinforcing wire with 200x200 mm mesh and upper supporting meshes of  $\text{Ø}4 \text{ S400C (Vr400)}$  with 100x150 mm mesh. In addition, the lower grid in the area of reduced thickness is reinforced with individual  $\text{Ø}8 \text{ S500 (A-500C)}$  with a spacing of 400 mm, as well as in the slab installed vertical V-shaped meshes with longitudinal reinforcement of  $3\text{Ø}5 \text{ S200C (Vr200)}$  and transverse bars  $3\text{Ø}4 \text{ S200C (Vr200)}$  with a spacing of 200 mm, installed with a spacing of 1.0-1.05 meters. The ceiling slab was loaded with small piece weights (bricks), the columns of which with dimensions of 500x500 mm were placed on a layer of sand in such a way as to exclude their mutual touching and formation of vaults (Figure 2).



Figure 2 – Loading the ceiling slab with brick columns

In the process of loading, vertical displacements were measured using PAO-6 deflection meters with a division value of 0.01 mm in the middle part of the span and at the supports (Figures 3 and 4), and the crack development pattern was recorded with crack opening width measurement using MPB-3 microscope with a division value of 0.02 mm [12].

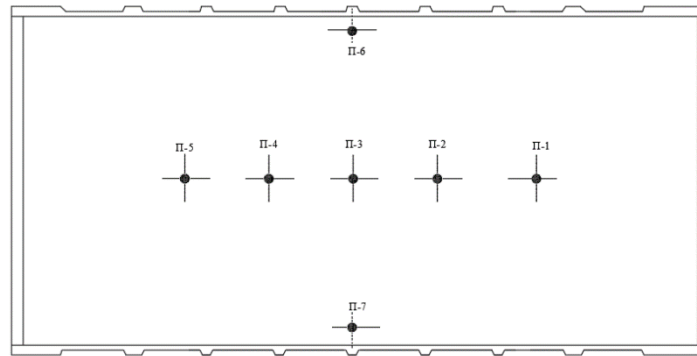


Figure 3 – Scheme of vertical deflection gauges on the ceiling slab



Figure 4 – Deflection gauges and safety supports under the ceiling slab

The reinforced concrete slabs under consideration are placed between two rows of volume blocks, forming an inter-block corridor in the building. The slabs have cantilevered overhangs, by which they rest on the projecting consoles of the volume blocks (Figure 5). Interblock floor slab is a flat reinforced concrete slab 140 mm thick, dimensions in plan 3480x2360 mm, made of heavy concrete class C20/25 (B25). The slab is reinforced with a bottom mesh of periodic profile reinforcement  $\varnothing 8$  S500 (A500C) and  $\varnothing 6$  S500 (B500C) with 200x200 mm cells and vertical frames with longitudinal reinforcement  $\varnothing 8$  S500 (A-500C) and transverse bars  $\varnothing 4$  B500 (B500C) located at the cantilever overhangs of the slab.

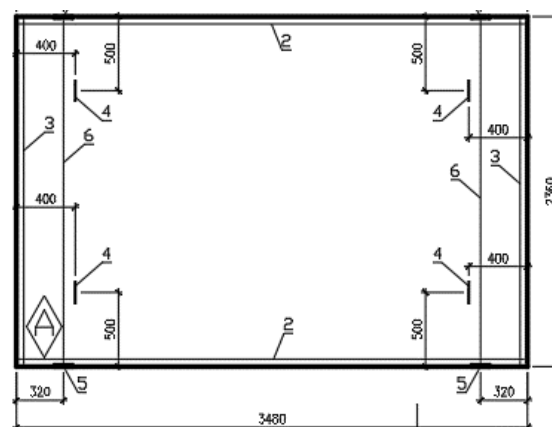


Figure 5 – Reinforcement of inter-corridor floor slab

Loading of the interblock ceiling slab with small piece weights (bricks), the columns of which with dimensions of 500x500 mm were placed on a layer of sand in such a way as to exclude their mutual touching and formation of vaults (Figures 6 and 7). In the process of loading of the

interlocking slab, vertical displacements were measured with the help of PAO-6 deflection gauges with a division value of 0.01 mm in the middle part of the span and on the supports (Figure 8).

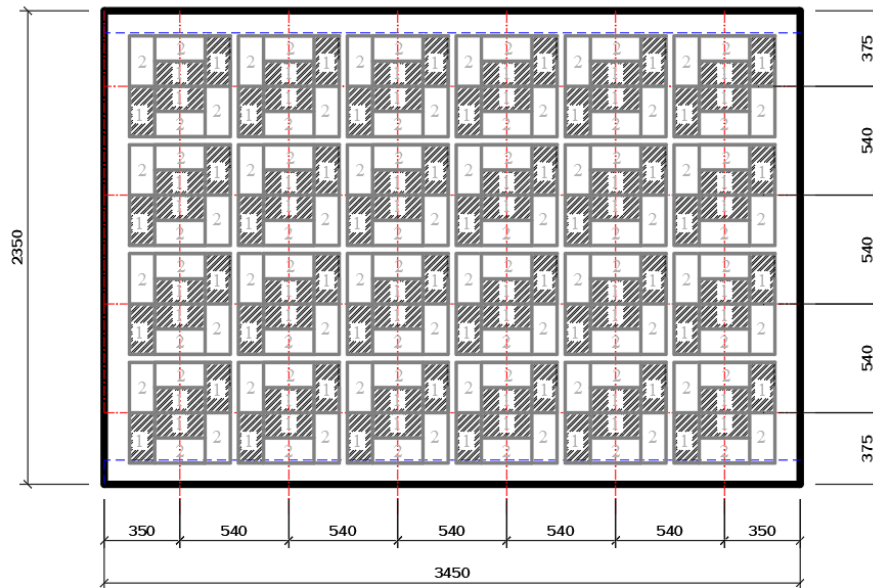


Figure 6 – Scheme of brick columns on the interlocking slab



Figure 7 – View of interlocking floor slab loaded with brick

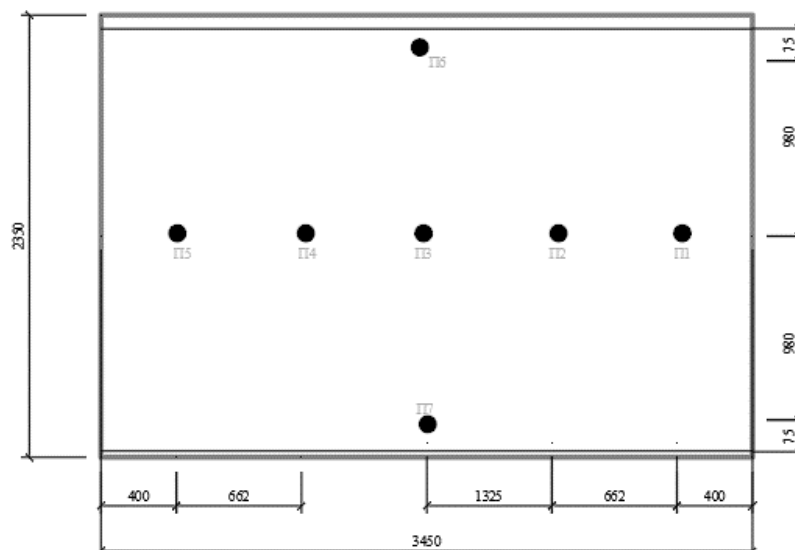


Figure 8 – Scheme of vertical deflection gauges on the interlocking slab



The picture of crack development was recorded by measuring the crack opening width using a microscope MPB-3 with a division value of 0.02 mm (Figure 9). The MPB-3 microscope provides an opportunity to enlarge the observation area and allows to study of the material structure at the micro level with a high degree of resolution. Measurement of crack opening width allows not only to monitor the development of cracks but also to assess the degree of their danger to the material. The greater the crack opening width, the more likely it is that the crack may lead to failure or fracture of the material.



Figure 9 – View of safety supports under the interblock corridor slab

### 3. Results and Discussion

Figure 10 shows the deflection pattern of the middle part of the ceiling slab, which shows a shift of the maximum deflections to the thinner part of the ceiling slab. The deflection at the variable load  $q_k = 70 \text{ kgf/m}^2$  was about 1.5 mm, which is significantly less than the allowable deflection (at  $f/l=1/200$  the allowable deflection is 15.6 mm),  $q_k = 582.3 \text{ kgf/m}^2$  the ceiling slab rested on the safety support, with a maximum deflection of 52.3 mm. Cracks in the ceiling slab appeared at a vertical load of  $240 \text{ kgf/m}^2$ , and before the ceiling slab failed, their opening width reached 0.9 mm (Figures 11 - 12). In general, the ceiling slab has sufficient stiffness, crack resistance, and strength.

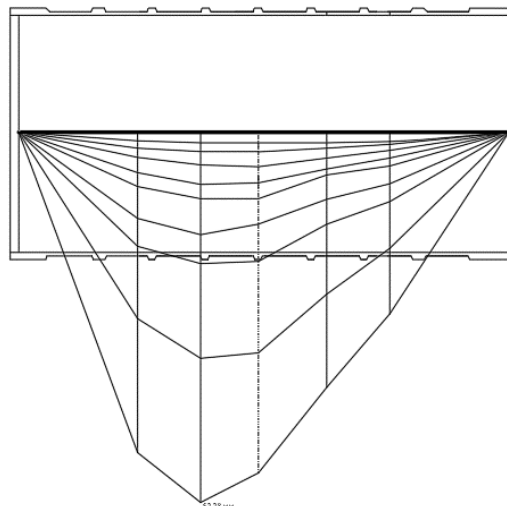


Figure 10 – Graph of vertical displacements of the middle part of the ceiling slab

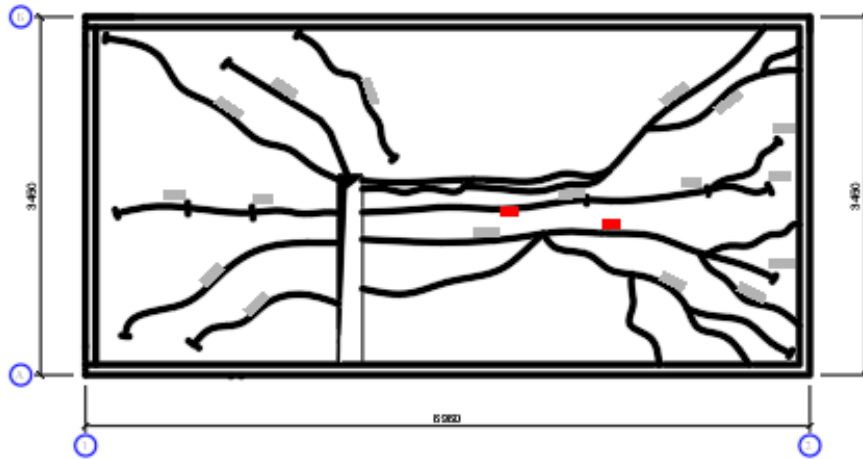


Figure 11 – Cracking pattern on the underside of the ceiling slab



Figure 12 – Cracks in the ceiling slab

The deflection at a variable load  $q_k = 3.0 \text{ kgf/m}^2$  was about 1.3 mm, which is significantly less than the allowable deflection (at  $f/l=1/200$  the allowable deflection is 11.4 mm). Cracks in the interlocking slab appeared at a vertical load of  $550 \text{ kg/m}^2$ , and before the failure of the interlocking slab, the width of their opening reached 1.7 mm (Figures 13 - 14).

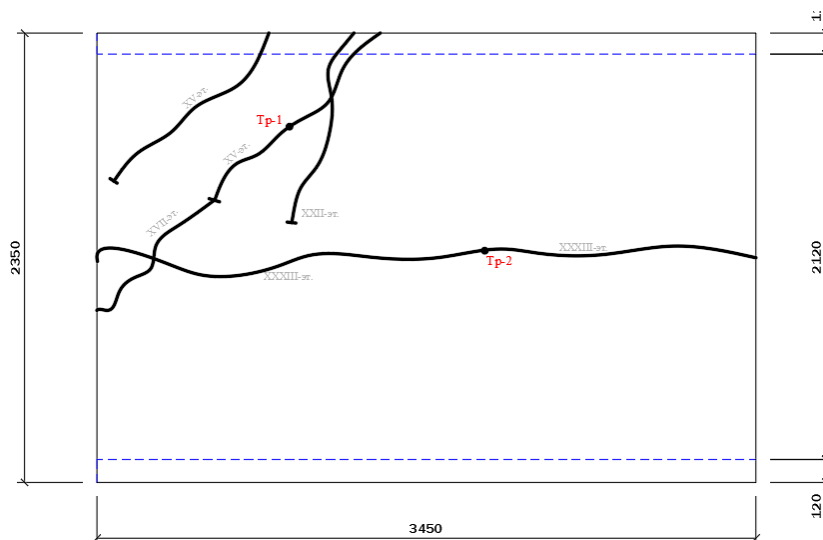


Figure 13 – Diagram of cracks in the interlocking floor slab



Figure 14 – Cracks in the interlocking floor slab

The failure of the inter-unit floor slab occurred at a vertical load  $q_k = 1510.5 \text{ kg/m}^2$ , which exceeds the control failure load according to [11] by almost two times. The largest deflection of the corridor slab before failure was 11 mm, indicating the high stiffness of the floor slab. In general, the interlocking floor slab has sufficient stiffness, crack resistance, and strength.

#### 4. Conclusions

The performed control tests of elements and assemblies of volumetric blocks allow us to draw the following conclusions:

1. The ceiling slabs unite the walls of the volume block as a single system and take vertical loads only from their weight.

–Damage to the expanded clay concrete ceiling slab under vertical loading is accompanied by the formation of envelope-shaped cracks on the bottom surface of the slab. The cracks in the slab appeared at loads exceeding the alternating load. The deflections under alternating load were about 1.5 m, which is significantly less than the allowable deflection.

–Damage to the expanded clay concrete ceiling slab under vertical loading is accompanied by the formation of envelope-shaped cracks on the bottom surface of the slab. The cracks in the slab appeared at loads exceeding the alternating load. The deflections under alternating load were about 1.5 m, which is significantly less than the allowable deflection.

–The failure of the ceiling slab was accompanied by a significant crack opening, with the value of the experimental failure load exceeding the control failure load. The crack opening width reached 0.9 mm, and the vertical deflections exceeded 50 mm.

–The test results of the ceiling slab indicate that it is sufficiently strong, stiff, and crack-resistant.

2. The floor slab of the inter-unit corridor is designed to accept variable vertical loads and to unite parallel rows of modular units into a single system.

–The reinforced concrete slab of the inter-block corridor under vertical loading acts as a single-span spherically supported slab, in which the main crack runs in the middle part of the span and reaches 1.7 mm before failure. The deflections of the slab under alternating load were less than the allowable deflections and the first cracks were formed by the vertical load exceeding the alternating loads.

–The failure load in the inter-unit corridor floor slab was almost twice the control failure load, and the pre-failure deflection was about 11 mm.

–In general, the floor slab of the inter-unit corridor meets the requirements of the standards for strength, stiffness, and crack resistance.

## References

1. Innovative concrete concepts for design and construction of buildings / Colaco, JP // Proceedings of the first international conference on recent advances in concrete technology. — 2007. — P. 321–328.
2. Strength and deformations of volume-blocks / Bespaev, A., Teshev, I., Kuralov, U.S., Altigenov, U.B. // Smart Geotechnics for Smart Societies. — 2023. — P. 2408–2412.
3. Quantitative and Qualitative Analysis of Applying Building Information Modeling (BIM) for Infrastructure Design Process / M.-H. Shin, J.-H. Jung, H.-Y. Kim // Buildings. — 2022. — Vol. 12, No. 9. — P. 1476. <https://doi.org/10.3390/buildings12091476>
4. BIM-based simplified approach to automatically estimate building costs for projects in Thailand / S. Tokla // International Journal of GEOMATE. — 2020. — Vol. 18, No. 68. <https://doi.org/10.21660/2020.68.5777>
5. A Strategy for Building Design Quality Improvement through BIM Capability Analysis / H.J. Koo, J.T. O'Connor // Journal of Construction Engineering and Management. — 2022. — Vol. 148, No. 8. — P. 04022066. [https://doi.org/10.1061/\(ASCE\)CO.1943-7862.0002318](https://doi.org/10.1061/(ASCE)CO.1943-7862.0002318)
6. Production / Elkon [Electronic resource]. — 2024. — URL: <https://www.elkon.net> (date of access 15.02.2024).
7. Products / Bostadsbolaget [Electronic resource]. — 2024. — URL: <https://bostadsbolaget.se/english> (date of access 15.02.2024).
8. The Function and Potential of Innovative Reinforced Concrete Prefabrication Technologies in Achieving Residential Construction Goals in Germany and Poland / P. Kirschke, D. Sietko // Buildings. — 2021. — Vol. 11, No. 11. — P. 533. <https://doi.org/10.3390/buildings11110533>
9. Monitoring reinforced concrete building structure technical conditions based on the use of quasi-distributed fiber-optic sensors / A. Mekhtiyev // International Journal of GEOMATE. — 2022. — Vol. 23, No. 97. <https://doi.org/10.21660/2022.97.3392>
10. Tehnicheskij otchet o kontrolnyh ispytaniyah elementov i uzlov obemnyh blokov v g. Nur-Sultan / AO "KazNIISA" — 2020.
11. GOST 8829-94 Reinforced concrete and prefabricated concrete building products. Loading test methods. Assessment of strength, rigidity and crack resistance. — 1994. — 35 p.
12. ST RK EN 12390-1 Testing of fresh concrete - Part 3: Compressive strength testing. — 2016. — 30 p.

## Information about authors:

*Ulan Altigenov* – PhD Student, Department of Civil Engineering, L.N. Gumilyov Eurasian National University, Astana, Kazakhstan, [860806301721@enu.kz](mailto:860806301721@enu.kz)

*Aliy Bespaev* – Doctor of Technical Sciences, Professor, Kazakh Scientific Research and Design Institute of Civil Engineering and Architecture, JSC, Almaty, Kazakhstan, [aliy40@mail.ru](mailto:aliy40@mail.ru)

*Natalya Ryvkina* – Senior Lecturer, Department of Civil Engineering, L.N. Gumilyov Eurasian National University, Astana, Kazakhstan, [rondv2@mail.ru](mailto:rondv2@mail.ru)

*Ilya Teshev* – PhD Student, Department of Civil Engineering, Satbayev University, Almaty, Kazakhstan, [teshev.i@stud.satbayev.university](mailto:teshev.i@stud.satbayev.university)

## Author Contributions:

*Ulan Altigenov* – concept, testing, modeling, funding acquisition.

*Aliy Bespaev* – methodology, testing, visualization.

*Natalya Ryvkina* – editing.

*Ilya Teshev* – analysis, interpretation.

*Received: 24.02.2024*

*Revised: 19.03.2024*

*Accepted: 19.03.2024*

*Published: 19.03.2024*



## Research of foam concrete quality by two-stage foam injection method in comparison with classical foam concrete

Rauan Lukpanov<sup>1,2</sup>, Duman Dyusseminov<sup>1,2</sup>, Aliya Altynbekova<sup>1,2,\*</sup>,  
 Zhibek Zhantlesova<sup>1,2</sup>, Tattigul Seidmarova<sup>2</sup>

<sup>1</sup>Solid Research Group, LLP, 010008, Tashenova str., 23, Astana, Kazakhstan

<sup>2</sup>Department of Technology of Industrial and Civil Engineering, L.N. Gumilyov Eurasian National University, 010008, Satpayev str., 2, Astana, Kazakhstan

\*Correspondence: [proyekt.2022@bk.ru](mailto:proyekt.2022@bk.ru)

**Abstract.** The article presents a method of production of foam concrete, which involves two-stage injection of foam. The proposed method involves improving the pore structure of foam concrete, due to a more uniform distribution of pores throughout the volume of the material. Laboratory tests were carried out for two types of samples, represented by the proposed method of foam concrete production by two-stage foam injection with the use of modified additive in comparison with the classical foam concrete. The density of Type 1 samples varies from 410 to 793 kg/m<sup>3</sup> (coefficient of variation from 5.12 to 7.31%), while the density of fiberboard samples lies within the range from 539 to 655 kg/m<sup>3</sup> (coefficient of variation from 2.66 to 3.14%). The results of greater variation of densities by height in the Type 1 sample relative to the Type 2 sample indicate the influence of the technological process of foam concrete production on the quality of the pore structure of the material. The results of strength evaluation showed a large scatter of Type 1 samples in relation to Type 2 samples. The highest values of CM strengths are logically observed in the lower part of the sample and the lowest in the upper location: 44.04 and 32.33 kg/cm<sup>2</sup> (coefficient of variation from 5.15 to 9.54%). For Type 2 samples, the same values are 55.18 and 44.44 kg/cm<sup>2</sup>, for the lower and upper locations, respectively (coefficient of variation from 2.79 to 5.35%). The results of thermal conductivity measurements of Type 1 samples range from 0.098 to 0.203 W/m<sup>0</sup>C (coefficient of variation from 4.59 to 11.88%), while the densities of Type 2 samples lie between 128 and 162 W/m<sup>0</sup>C (coefficient of variation from 3.38 to 3.55%).

**Keywords:** foam concrete, blowing agent, microsilica, post-alcohol bard, density, strength, thermal insulation properties, production technology.

### 1. Introduction

In recent decades, intensive research in the field of concrete has led to significant progress in both theoretical aspects and technological developments. This includes the development of new admixtures, the optimization of compositions and mixing techniques, and the application of specialized processing and curing methods. These efforts have made possible the creation and production of concretes with a wide range of properties, from heavy to lightweight, with unique characteristics of strength, durability, thermal and acoustic insulation, and the ability to adapt to different operating conditions and environments [1-3].

In modern conditions, there is an active development of foam concrete production, which is due to the introduction of new, more efficient blowing agents and the use of energy-saving technologies based on the principles of non-autoclave production. New blowing agents offer more precise control over the process of foam formation, which allows to obtain more stable product quality and reduce production costs [4-6].

The development of new approaches to foam concrete production is an integral part of the evolution in the construction industry. Modern production methods face challenges such as



structure heterogeneity and material shrinkage during the setting process [7, 8]. Despite the progress, shrinkage remains an issue as it can influence the final properties of building products. Nevertheless, the classical production method continues to be widely used in the construction industry, with the constant introduction of various additives and improvements. The continuous search for new foam concrete production methods is driving innovation in the construction industry. This search is aimed at improving the quality of building materials and providing increased efficiency and durability of building structures in general [9-11].

To solve the problems associated with instability of structure and non-uniformity of foam concrete density, an approach based on two-stage introduction of foam into the material is proposed. The initial introduction of a low-concentrated blowing agent solution allows to achieve uniform foam distribution within the mixture. This helps to create a more homogeneous and stable material structure. This is followed by the addition of a highly concentrated solution, which further enhances the formation of a stable foam concrete structure. This approach ensures that the foam is evenly distributed in the material, making the final product more homogeneous and stable. Reducing the water-cement ratio at the production stage shortens the setting time, which in turn improves the strength characteristics of the foam concrete. These results are confirmed by numerous studies in the field of construction materials and technologies [12-24].

Foam concrete producers are regularly challenged by structural instability, material shrinkage and uneven density, which can ultimately affect the stability and quality of the finished product. These deficiencies are often caused by high water-cement ratios, which affect the texture and overall quality characteristic of the concrete. To solve these problems, producers resort to the use of plasticizing admixtures, which not only improve the mortar characteristics but also achieve more stable results in production [25, 26]. The addition of various modifying admixtures makes it possible to customize the properties of concrete according to the requirements and improve its performance, providing more durable and better quality end products. Modified admixtures and plasticizers represent an integral part of the foam concrete improvement process in the construction industry. Research and experimental applications of these additives demonstrate their significant contribution in strengthening the structure, reducing material shrinkage and providing uniform density. These factors significantly improve the strength and thermal insulation properties of foam concrete, making it a more competitive and sought-after material for various construction applications. However, it is important to note that when choosing modified additives and plasticizers it is necessary to take into account not only their technical characteristics, but also their environmental impact [27-29].

The developed modified additive for foamed concrete includes two key components: microsilica and post-alcohol bard. Microsilica, which is a finely dispersed substance, helps to improve the strength and stability of the material structure, as well as to increase its thermal insulation properties by optimizing the internal structure. Post-alcohol bard, in turn, has properties that help to increase density and improve adhesion, which affects the durability and stability of foam concrete. The combination of these ingredients creates an effective additive that can improve the quality and performance of foam concrete, making it a stronger, more thermally insulating and durable material for building structures. Both of these components are important ingredients for creating high quality foam concrete with improved performance.

The aim of the study is to evaluate the homogeneity of the pore structure of the proposed method of foam concrete production by two-stage foam injection using a modified additive in comparison with classical foam concrete.

## **2. Methods**

In order to realize the set goal it is necessary to solve the following tasks:

- to prepare large samples of foam concrete produced by the classical method and the two-stage foam injection method, GOST 25485-2019, GOST17177-94 [30, 31];

- to prepare samples by segmenting large samples and taking them from different locations for further laboratory testing, GOST 25485-2019, GOST17177-94 [30, 31];
- laboratory testing of foam concrete samples to determine the density, strength and thermal insulation values (Figure 1), GOST 25485-2019, GOST17177-94 [30, 31].



Figure 1 – Laboratory testing of foam concrete

From the technological point of view, the proposed production method is fundamentally different from the previous technologies and includes two-stage foam injection, which was not practiced earlier (Figure 2). The proposed method provides maximum distribution of foam concentrate over the entire volume of the sample: the primary introduction of low-concentrated foam solution occurs at the stage of preparation of sand-cement mortar, thereby improving its wettability and subsequent reduction of water-cement ratio (reducing foam quenching by water). Subsequently, at the secondary introduction of highly concentrated foam solution at the stage of manufacturing the structure of cellular concrete, the reduction of water-cement ratio allows to maximally preserve the primary multiplicity of foam concentrate, contributes to the formation of a uniform structure of porous material.

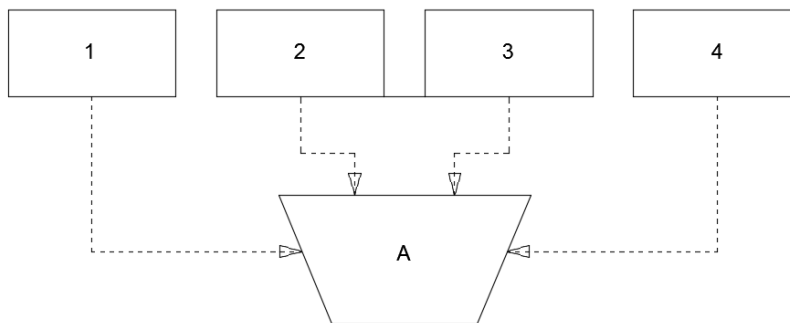


Figure 2 - Scheme of foam concrete production by two-stage foam injection

The technological process is represented by the following production stages: stage 1 - introduction of microsilica with post-alcohol bard, in the ratio of 10:1 by mass (60 kg per 6 liters per 1 cube), kneading 5 minutes; stage 2 - introduction of sand-cement mixture, in the ratio of sand to cement 1: 1.40-1.45 by weight (220 kg to 320 kg per 1 cube), kneading 2-3 minutes; stage 3 - introduction of foam with water in the ratio of 0.23 grams of foam per 75 liters of water per 1 cube, kneading 5 minutes; stage 4 - leading foam with water in the ratio of 1.27 grams of foam per 40 liters of water per 1 cube, kneading 2 minutes.

The studies will be performed for foam concrete samples made by the proposed method of two-stage introduction of foam with additive. The results will be compared with the reference

sample - with the classical foam concrete production technology. The technological composition of manufacturing of each method is presented in Table 1.

Table 1 – Technological composition of the compared samples

Index	Unit	Type 1	Type 2
Microsilica	kilogram	-	-
M400 cement	kilogram	320	320
Fine sand	kilogram	220	220
Post-alcohol bard	liter	-	6
Foaming agent to water ratio at primary injection	gram : liter	1.5:115	0.23:75
Foaming agent to water ratio at secondary injection	gram : liter	-	1.27:40

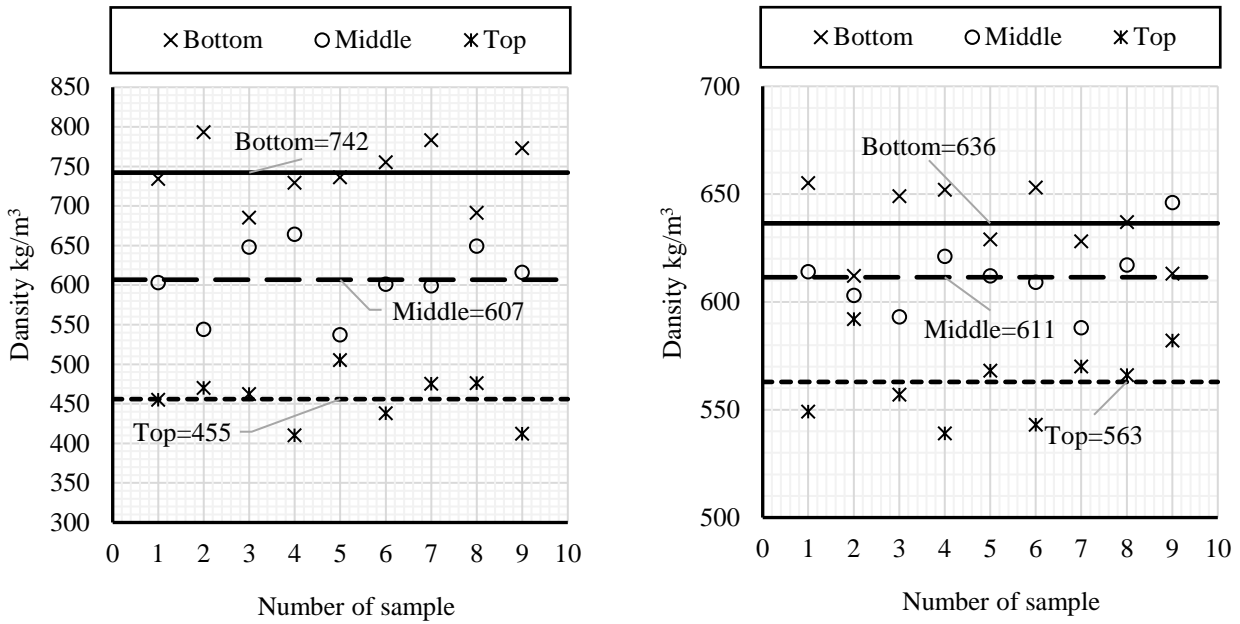
A total of 6 samples were tested for each of the compared types of foam concrete samples in order to obtain statistical measurement data. To evaluate the quality of pore structure of foam concrete, a large cube-shaped sample with dimensions 500x500 mm was prepared. To assess the volumetric homogeneity (distribution of pores throughout the volume of the material), the large sample was segmented into cubes (samples) with dimensions 100x100 mm. Control sampling for evaluation of physical-mechanical and strength characteristics was performed in the middle and peripheral (upper and lower) parts of the sample. The variability of sampling in the vertical direction is primarily due to the fact that the heterogeneity of the pore structure of foam concrete is manifested in the vertical direction. The latter is due to the fact that during foam quenching the formed soapy water tends downward, under the influence of gravitational forces, until the setting of the cement-sand mixture. Therefore, analyzing the vertical distribution of the pore structure is the prerogative of this study. The vertical variation in sampling, however, is primarily due to the statistical necessity required to obtain a stable average result. For convenience, the samples were labeled, vertically with Latin letters and horizontally with Arabic and Roman numerals. A total of 27 samples were collected, 9 samples from each distinct vertical level.

### 3. Results and Discussion

Figure 3 shows the results of density determinations of the compared foam concrete samples. Figure 3a shows the results of partial values of classical foam concrete (Type 1), Figure 3b - of foam concrete with two-stage foaming (Type 2).

According to the measurement results, the Type 1 samples show a significant vertical variation in density values. Samples from the lower part of the Type 1 sample showed the highest values, ranging from 685 to 793 kg/m<sup>3</sup>, with an average value of 742 kg/m<sup>3</sup>. The lowest density values were found in the upper part of the large sample: 410 to 505 kg/m<sup>3</sup>, with an average value of 455 kg/m<sup>3</sup>. In the middle part of the sample, the density is maximally consistent with the D600 foam concrete grade, ranging from 537 to 664 kg/m<sup>3</sup>, with an average value of 607 kg/m<sup>3</sup>. Relatively dense density results are observed in Type 2 samples. The densities in the lower part range from 612-655 kg/m<sup>3</sup> and the average is 636 kg/m<sup>3</sup>. The densities in the lower part are in the range of 539-592 kg/m<sup>3</sup> and the average is 563 kg/m<sup>3</sup>. The density results in the middle part, also maximally corresponding to the D600 foam concrete grade, ranges from 588 to 617 kg/m<sup>3</sup>, and the average is 611 kg/m<sup>3</sup>. Comparison of the coefficients of variation showed that the stability of the private values of Type 1 samples is much lower than Type 2 samples. The variation of Type 1 samples ranges from 5.12 to 7.31% while that of type 2 samples ranges from 2.66 to 3.14%. The maximum variation of data of Type 1 samples is 50% higher than that of Type 2 samples. Nevertheless, the relationship of the individual values remains close as the maximum variation values do not exceed 10%.

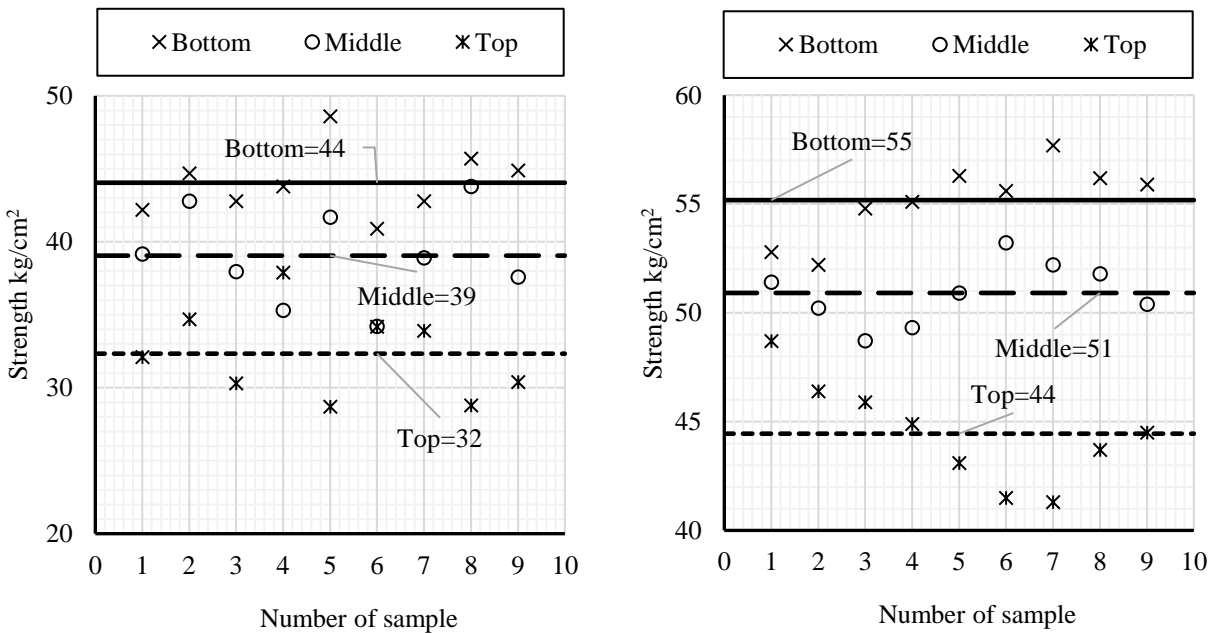
The results of a greater variation of densities by height in the sample of Type 1 relative to the sample of Type 2 indicates the influence of the technological process of foam concrete production on the quality of the pore structure of the material.



a) Values of classical foam concrete      b) Values of foam concrete with two-stage foaming

Figure 3 – Results of density measurements

Figure 4 shows the results of determinations of strength values of the compared foam concrete samples. Figure 4a shows the results of private values of Type 1 foam concrete, Figure 4b – Type 2 foam concrete.



a) Results of Type 1      b) Results of Type 2

Figure 4 – Results of strength measurements

Figure 5 shows the results of determinations of thermal conductivity values of the compared foam concrete samples. Figure 5a shows the results of partial values of Type 1 foam concrete, Figure 5b – Type 2 foam concrete.

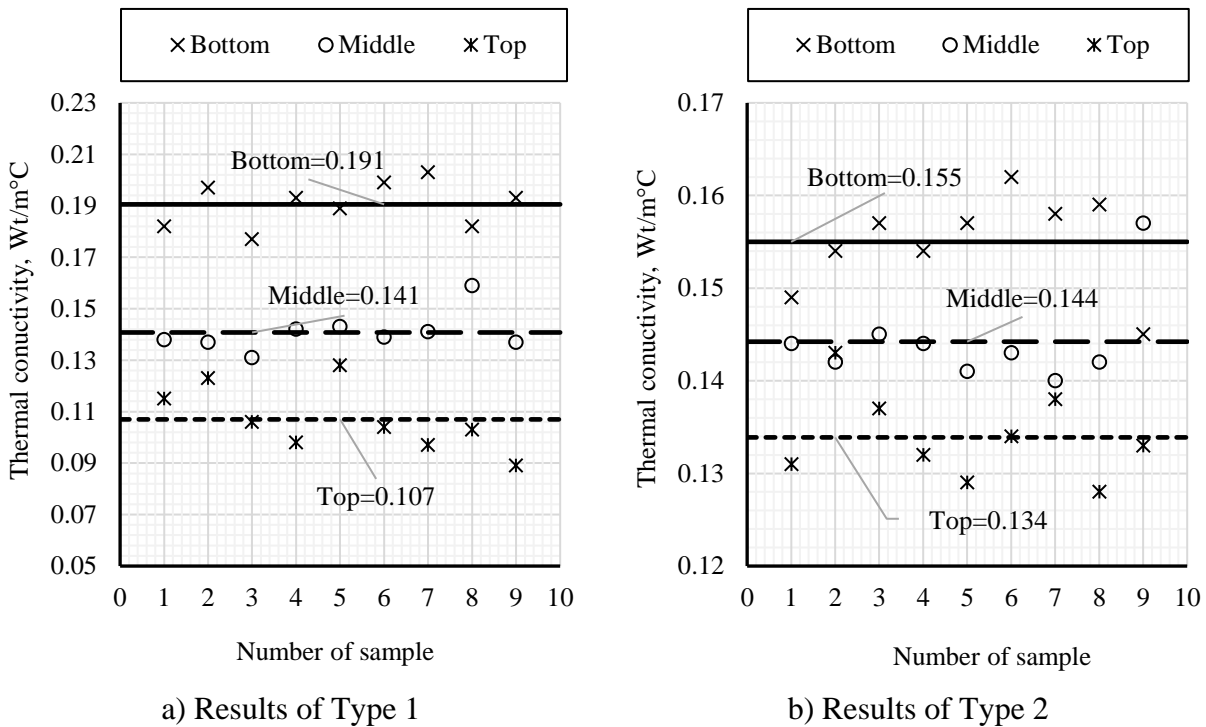


Figure 5 – Results of thermal conductivity measurements

The results of thermal conductivity measurements logically showed a similar dependence with the estimation of densities: the Type 1 samples show a significant vertical variation of values. The highest values are also observed in the lower part of the sample, which corresponds to the maximum density: thermal conductivity varies from 0.177 to 0.203  $\text{W/m}^0\text{C}$ , with an average value of 0.191  $\text{W/m}^0\text{C}$ . The lowest thermal conductivity values are logically found in the upper part of the large sample, which corresponds to the lowest thermal conductivity values: 0.098 to 0.159  $\text{W/m}^0\text{C}$ , with an average value of 0.107  $\text{W/m}^0\text{C}$ . In the middle part of the sample, the thermal conductivity varies from 0.131 to 0.159  $\text{W/m}^0\text{C}$ , with an average value of 0.141  $\text{W/m}^0\text{C}$ . In the lower part of the type 2 image, the thermal conductivity ranges from 0.145-0.162  $\text{W/m}^0\text{C}$  and the average strength is 0.155  $\text{W/m}^0\text{C}$ . The thermal conductivity in the lower part of the sample ranges from 0.128-0.143  $\text{W/m}^0\text{C}$  and the average strength is 0.134  $\text{W/m}^0\text{C}$ . The results of thermal conductivity in the middle part varies from 0.140 to 0.157  $\text{W/m}^0\text{C}$ , and the average is 0.144  $\text{W/m}^0\text{C}$ .

Comparison of coefficients of variation showed that the stability of private values of Type 1 samples, as in the case of density, is significantly lower than that of Type 2 samples. The variation of Type 1 samples ranges from 4.59 to 11.88%, while that of type 2 samples ranges from 3.38 to 3.55%. The maximum data variation of Type 1 samples is more than 50% higher than that of Type 2 samples. The results of greater variation of thermal conductivity, as in the case of density, by height in sample type 1 relative to sample Type 2 indicates the influence of the technological process of foam concrete production on the quality of the pore structure of the material.

#### 4. Conclusions

The following conclusions can be made on the basis of the experimental studies:

1. The results of density estimation of segmented foam concrete samples produced by the classical method (Type 1) and the two-stage foam injection method (Type 2) were obtained. The results showed a non-uniform distribution of the pore structure of foam concrete in the vertical of the Type 1 samples relative to the Type 2. A large variation in the density of Type 1 is particularly observed in the vertical, where the lower samples showed densities on average 38% higher than those of the upper location samples. The same figure for the fiberboard samples was, on average, only 11%. The density of the Type 1 samples ranged from 410 to 793  $\text{kg/m}^3$  (coefficient of



variation from 5.12 to 7.31%), while the density of the fiberboard samples ranged from 539 to 655 kg/m<sup>3</sup> (coefficient of variation from 2.66 to 3.14%). The results of greater variation of densities by height in the sample of Type 1 relative to the sample of Type 2 indicate the influence of the technological process of foam concrete production on the quality of the pore structure of the material.

2. The results of strength evaluation of the same segmented foam concrete samples were obtained. The results expectedly showed a large variation of Type 1 samples with respect to the fiberboard samples. The highest values of Type 1 strengths are logically observed in the lower part of the sample and the lowest in the upper location: 44.04 and 32.33 kg/cm<sup>2</sup> (coefficient of variation from 5.15 to 9.54%). For fiberboard samples, the same values are 55.18 and 44.44 kg/cm<sup>2</sup>, for the lower and upper locations, respectively (coefficient of variation from 2.79 to 5.35%). The maximum variation of Type 1 sample data is 40% higher than the variation of Type 2 sample data. All private strength values of Type 2 samples exceed the private strength values of Type 1 samples (regardless of location), which is not characteristic of previously determined material density in different locations. The latter indicates the influence of the modified additive on the strength values of foam concrete.

3. The results of thermal conductivity estimation of the same segmented foam concrete samples were obtained. The results of thermal conductivity measurements logically showed a similar relationship with the estimation of densities: the Type 1 samples have a significant vertical scatter of values. In percentage terms, the scatter of Type 1 thermal conductivity is as follows: the thermal conductivity of the lower location samples is on average 44% higher than the thermal conductivity of the upper location samples. The same indicator for fiberboard samples was only 13%. The thermal conductivity of Type 1 samples varies from 0.098 to 0.203 W/m<sup>0</sup>C (coefficient of variation from 4.59 to 11.88%), while the density of fiberboard samples lie in the range from 128 to 162 W/m<sup>0</sup>C (coefficient of variation from 3.38 to 3.55%). The results of greater variation of thermal conductivity, as well as in the case of density, by height in the sample of Type 1 relative to the sample of Type 2 indicates the influence of the technological process of foam concrete production on the quality of the pore structure of the material.

### Acknowledgments

This research was funded by the Science Committee of the Ministry of Education and Science of the Republic of Kazakhstan (Grant № AP13068424).

### References

1. Cellular concrete review: New trends for application in construction / L. Chica, A. Alzate, // Construction and building materials. — 2019. — Vol. 200. — P. 637-647.
2. Materials production, properties and application of aerated lightweight concrete: review / A.J. Hamad // International journal of materials science and engineering. — 2014. — Vol. 2. — No. 2. — P. 152-157.
3. Waterproof performance of concrete: A critical review on implemented approaches / N.Z. Muhammad, A. Keyvanfar, M.Z. Abd. Majid, A. Shafaghat, J. Mirza // Construction and Building Materials. — 2015. — Vol. 101, No. 1. — P. 80–90. <https://doi.org/10.1016/j.conbuildmat.2015.10.048>
4. Kak prevratit betony starogo pokoleniya v vysokoeffektivnye betony novogo pokoleniya / V.I. Kalashnikov // Beton i zhelezobeton. — 2012. — Vol. 1. No. 1. — P. 82–89.
5. Handbook of foaming and blowing agents / G. Wypych. — Toronto: ChemTec Publishing, 2017. — 250 p.
6. Experimental investigation on cement-based foam developed to prevent spontaneous combustion of coal by plugging air leakage / X. Xi, S. Jiang, C. Yin, Z. Wu // Fuel. — 2021. — Vol. 301. — P. 121091. <https://doi.org/10.1016/j.fuel.2021.121091>
7. Effektivnoe modifizirovanie sistem tverdeniya cementnogo kamnya s ispolzovaniem aktivirovannogo mikroremnezema / M.S. Zakurazhnov, O.V. Artamonova, E.I. Shmitko // Izvestiya TulGU. Tehnicheskie nauki. — 2015. — Vol. 12, No. 1. — P. 43–52.
8. Kompleksnaya dobavka dlya cementnogo vyazhushhego / D.V. Shirshaeva, A.S. Ustyugov // Izbrannye doklady 65-j yubilejnoj universitetskoj nauchno-tehnicheskoy konferencii studentov i molodyh uchenyh. — Tomsk, Russia: TSUAB. — 2019. — P. 878–879.
9. Chemical Blowing Agent Systems for Polymer Foam Manufacture / C. O'Connor. — The University of Manchester, 1999.

10. Development of macro/nanocellular foams in polymer nanocomposites / S. Bhattacharya. — Melbourne: RMIT University, 2009. — 226 p.
11. Chemical admixtures — Chemistry, applications and their impact on concrete microstructure and durability / J. Plank, E. Sakai, C.W. Miao, C. Yu, J.X. Hong // Cement and Concrete Research. — 2015. — Vol. 78. No. 1. — P. 81–99. <https://doi.org/10.1016/j.cemconres.2015.05.016>
12. Research of foam concrete components in the regional production conditions of Nur-Sultan / Lukpanov, R., Dyusseminov, D., Altyzbekova, A., Zhantlesova, Z. // Technobius. — 2022. — Vol. 22(3). 0023. <https://doi.org/10.54355/tbus/2.3.2022.0023>
13. Influence of the technological foam concrete manufacturing process on its pore structure / Lukpanov, R., Dyusseminov, D., Shakhmov, Z., Bazarbayev, D., Tsygulyov, D., Yenkebayev, S. // Magazine of Civil Engineering. —2022. — Vol. 115(7). 11513. <https://doi.org/10.34910/MCE.115.13>
14. Composite non-autoclaved aerated concrete based on an emulsion / Yerlan, S., Duman, D., Adiya, Z., Daniyar, B., Rauan, L. // Magazine of Civil Engineering. —2021. — Vol. 6 (106). 10605. <https://doi.org/10.34910/MCE.106.5>
15. Approximative approach to optimize concrete foaming concentration in two stage foaming / Lukpanov, R., Dyusseminov, D., Zhantlessova, Z., Altyzbekova, A., Smoljaninov, A. // Technobius. —2023. — Vol. 3(3). 0041. <https://doi.org/10.54355/tbus/3.3.2023.0041>
16. Effect of a complex modified additive on the setting time of the cement mixture / Altyzbekova, A., Lukpanov, R., Dyusseminov, D., Askerbekova, A., Tkach, E. // Complex Use of Mineral Resources. —2022. — Vol. 325(2). — P. 29–38. <https://doi.org/10.31643/2023/6445.15>
17. Assessment of the physical and mechanical characteristics of sand for the production of foam concrete using the two-stage foam injection method / Lukpanov, R., Dyusseminov, D., Altyzbekova, A., Yenkebayev, S., Awwad, T. // Complex Use of Mineral Resources. —2024. — Vol. 332(1). — P. 5–18. <https://doi.org/10.31643/2025/6445.01>
18. Optimal concentration of post-alcohol bard and microsilica in cement-sand mixtures determination / Lukpanov, R., Dyusseminov, D., Altyzbekova, A., Yenkebayev, S., Awwad, T. // Complex Use of Mineral Resources. —2023. — Vol. 330(3). — P. 92–103. <https://doi.org/10.31643/2024/6445.33>
19. Complex laboratory studies of modified additive influence on concrete physical and mechanical properties / Altyzbekova, A., Lukpanov, R., Yenkebayev, S., Tsygulyov, D., Nurbayeva, M. // International Journal of GEOMATE. —2022. — Vol. 23(100). — P. 26–33. <https://doi.org/10.21660/2022.100.3641>
20. Research on the effect of microsilica on the properties of the cement-sand mixture / Lukpanov, R., Dyusseminov, D., Altyzbekova, A., Zhantlesova, Z. // Technobius. —2022. — Vol. 2(4). 0027. <https://doi.org/10.54355/tbus/2.4.2022.0027>
21. Complex modified additive for concrete based on industrial waste / Lukpanov, R., Dyusseminov, D., Tsygulyov, D., & Yenkebayev, S. // Magazine of Civil Engineering. —2022. — Vol. 115(7). 11507. <https://doi.org/10.34910/MCE.115.7>
22. Additive for improving the quality of foam concrete made on the basis of micro silica and quicklime / Lukpanov, R., Dyusseminov, D., Yenkebayev, S., Yenkebayeva, A., Tkach, E. // Complex Use of Mineral Resources. — 2022. — Vol. 323(4). — P. 30–37. <https://doi.org/10.31643/2022/6445.37>
23. Effect of a complex modified additive based on post-alcohol bard on the strength behavior of concrete / Altyzbekova, A., Lukpanov, R., Dyusseminov, D., Askerbekova, A., Gunasekaran, M. // Complex Use of Mineral Resources. —2023. — Vol. 327(4). — P. 5–14. <https://doi.org/10.31643/2023/6445.34>
24. Homogeneous pore distribution in foam concrete by two-stage foaming / Lukpanov, R. E., Dyusseminov, D. S., Bazarbayev, D. O., Tsygulyov, D. V., Yenkebayev, S. B. // Magazine of Civil Engineering. —2021. — Vol. 3 (103). 10313. <https://doi.org/10.34910/MCE.103.13>
25. Effects of ultrafine fly ash on the properties of high-strength concrete / F. Jingjing, L. Shuhua, W. Zhigang // Journal of Thermal Analysis and Calorimetry. — 2015. — Vol. 121, No. 1. — P. 1213–1223. <https://doi.org/10.1007/s10973-015-4567-3>
26. Modified Cement-Based Mortars: Crack Initiation and Volume Changes / I. Havlikova, V. Bilek, L. Topolar, H. Simonova, P. Schmid, Z. Kersner // Materials in Technology. — 2015. — Vol. 49, No. 4. — P. 557–561. <https://doi.org/10.17222/mit.2014.179>
27. Microstructure and mechanical properties of polymer-modified mortars / S. Marceau, F. Lespinasse, J. Bellanger, C. Mallet // European Journal of Environmental and Civil Engineering. — 2012. — Vol. 16, No. 5. — P. 571–581. <https://doi.org/10.1080/19648189.2012.675148>
28. Polymer-modified concrete with improved flexural toughness and mechanism analysis / C. Qingyu, S. Wei, G. Liping, Z. Guorong // Journal of Wuhan University of Technology-Materials Science Edition. . — 2012. — Vol. 27, No. 1. — P. 597–601. <https://doi.org/10.1007/s11595-012-0512-5>
29. Chemical admixtures—Chemistry, applications and their impact on concrete microstructure and durability / J. Plank, E. Sakai, C.W. Miao, C. Yu, J.X. Hong // Cement and Concrete Research. — 2015. — Vol. 78, No. 1. — P. 81–99. <https://doi.org/10.1016/j.cemconres.2015.05.016>
30. GOST 25485-2019 Cellular concretes. General specification. — 2019.
31. GOST 17177-94 Materials and products of building thermal insulation. Test methods. — 1994.

**Information about authors:**

*Rauan Lukpanov* – PhD, Scientific Supervisor, Solid Research Group, LLP, 010008, Tashenova str., 23, Astana, Kazakhstan. Professor, Department of Technology of Industrial and Civil Engineering, L.N. Gumilyov Eurasian National University, 010008, Satpayev str., 2, Astana, Kazakhstan, [rauan\\_82@mail.ru](mailto:rauan_82@mail.ru)

*Duman Dyusseminov* – Candidate of Technical Sciences, Senior Researcher, Solid Research Group, LLP, 010008, Tashenova str., 23, Astana Kazakhstan. Associate Professor, Department of Technology of Industrial and Civil Engineering, L.N. Gumilyov Eurasian National University, 010008, Satpayev str., 2, Astana, Kazakhstan, [duseminov@mail.ru](mailto:duseminov@mail.ru)

*Aliya Altynbekova* – Researcher, Solid Research Group, LLP, 010008, Tashenova str., 23, Astana, Kazakhstan. Senior Lecturer, Department of Technology of Industrial and Civil Engineering, L.N. Gumilyov Eurasian National University, 010008, Satpayev str., 2, Astana, Kazakhstan, [kleo-14@mail.ru](mailto:kleo-14@mail.ru)

*Zhibek Zhantlesova* – Junior Researcher, Solid Research Group, LLP, 010008, Tashenova str., 23, Astana, Kazakhstan. PhD Student, Department of Technology of Industrial and Civil Engineering, L.N. Gumilyov Eurasian National University, 010008, Satpayev str., 2, Astana, Kazakhstan, [zhibek81@mail.ru](mailto:zhibek81@mail.ru)

*Tattigul Seidmarova* – PhD, Senior Lecturer, Department of Technology of Industrial and Civil Engineering, L.N. Gumilyov Eurasian National University, 010008, Satpayev str., 2, Astana, Kazakhstan, [titi.gold1506@gmail.com](mailto:titi.gold1506@gmail.com)

**Author Contributions:**

*Rauan Lukpanov* – analysis, funding acquisition.

*Duman Dyusseminov* – concept, methodology.

*Aliya Altynbekova* – resources, data collection, modeling.

*Zhibek Zhantlesova* – editing, testing, visualization.

*Tattigul Seidmarova* – interpretation, drafting.

*Received: 18.02.2024*

*Revised: 20.03.2024*

*Accepted: 21.03.2024*

*Published: 21.03.2024*



## Geotechnical interpolation methodology for determining intermediate values of soil properties

Aliya Aldungarova<sup>1,2</sup>, Assel Mukhamejanova<sup>3,\*</sup>, Nurgul Alibekova<sup>1,3</sup>, Sabit Karaulov<sup>1</sup>,  
 Daniyar Akhmetov<sup>4</sup>

<sup>1</sup>Solid Research Group, LLP, Astana, Kazakhstan

<sup>2</sup>School of Architecture, Construction and Energy, D. Serikbayev East Kazakhstan Technical University, Ust-Kamenogorsk, Kazakhstan

<sup>3</sup>Department of Civil Engineering, L.N. Gumilyov Eurasian National University, Astana, Kazakhstan

<sup>4</sup>Department of Construction and Building Materials, Satbayev University, Almaty, Kazakhstan

\*Correspondence: [assel.84@list.ru](mailto:assel.84@list.ru)

**Abstract.** The article considers the application of geotechnical interpolation using ArcGIS software to determine the intermediate geotechnical properties of soils at a construction site in a residential complex in Astana, Esil district. The study is based on data from 8 boreholes drilled to a depth of 26 meters, and the purpose of the work is to use the kriging interpolation method to determine intermediate soil properties. The raw data include the results of analyzing the physical and mechanical properties of the soils from the boreholes, which served as a basis for interpolation and mapping. The results of the study are presented in the form of maps showing the intermediate mechanical properties of the soil at depths of 5, 10 and 15 m. The maps allow obtaining more accurate intermediate values. The proposed methodology not only facilitates the work of designers, but also provides data for realistic scenarios of soil strength and deformation characteristics, which significantly influences the selection of optimal types and sizes of foundations.

**Keywords:** geotechnical interpolation, ArcGIS software, Kriging, GIS, geotechnical engineering conditions, design optimization, data visualization.

### 1. Introduction

Over the past two decades, the development of geographic information systems (GIS) has led to their use for collecting, monitoring and analyzing geospatial data, providing a platform for combining different types of data and organizing information in visualizations using maps and 3D, allowing data to be stored, shared, analyzed and modified based on their actual location and requirements [1].

Geotechnical investigations play a key role in the civil engineering process but are often neglected due to various reasons such as ignorance, negligence or financial constraints [2].

However, geotechnical data collected by various organizations can be effectively used through GIS to map the geotechnical properties of the soil in an area, which helps reduce the time and cost of analysis and reduce construction delays [3].

GIS plays a critical role in developing data management systems to centrally store various soil properties and also facilitates data visualization and interpretation, making it a valuable tool for geotechnical engineering projects [4].

ArcGIS provides spatial analytics tools for interpolating data and identifying unknown data points, integrates with different domains depending on project requirements, is used by researchers to analyze location-based aspects such as land use and change detection, serves to store and manage

geotechnical data, and enables the creation of three-dimensional data models, enhancing visualization and analysis capabilities in geotechnical projects [5].

The use of geotechnical data, including soils maps and zoning through ArcGIS, helps reduce the cost and time of engineering projects by guiding site investigation and preliminary design, emphasizing the importance of understanding subsurface conditions, such as soil type and resistance, to safely and economically complete a project, and highlights the potential of spatial geotechnical data in planning site investigations and informing foundation design, while recognizing the need to [6].

This paper [7] discusses a method to account for the spatial variability of soil properties in geotechnical design using random fields based on cone penetration test (CPT) data, which provides a more accurate representation of in-situ soil variability and makes efficient use of available field data, and investigates the effect of the number of CPT measurements on reducing spatial uncertainty and the optimal interval between CPT measurements to reduce this uncertainty.

Article [8] presents a GIS implementation for geotechnical data management in Athens, Greece, describing the integration of data from more than 2,000 exploration wells and test pits to create thematic maps with geotechnical engineering information, and a methodology for automated seismic microzonation of the southern part of the city based on GIS and multiple data sources to assess seismic ground motion variability.

The paper [9] investigates the use of GIS to create interpolated geotechnical zoning maps in Surfers Paradise, Australia, based on data from 35 locations and 1,754 soil stiffness values, where interpolation methods including IDW, kriging and spline were evaluated using ArcMap10, showing that IDW provides the best representation for zoning maps to facilitate decision making for geotechnical projects in the region.

The results of the study [8] emphasize the effectiveness of GIS-based systems in mapping soil properties, which provides valuable information for planning and preliminary design of construction and engineering projects. In addition, the system helps to identify areas suitable for development and areas with potential problems, which facilitates informed decision-making in feasibility studies and future development planning.

A study on creating spatial soil maps from geotechnical data revealed that maps produced using the IDW method in ArcGIS can be an important tool for engineers, providing rapid assessment of soil properties at various depths and improving the safety and cost-effectiveness of projects by developing models of soil conditions at new sites [10].

In this study, we used the kriging method and ArcGIS software to assess the geotechnical properties of soils in Astana, which allowed us to create a methodology for determining intermediate strength and deformation properties with useful information for future projects and construction planning. The purpose of the study is to apply the method of kriging interpolation in ArcGIS software to determine the intermediate geotechnical properties of soil at the construction site in a residential complex in Astana.

## **2. Methods**

The study area is a residential complex in Astana city in Yesil district. Street E 116. Topographic survey at a scale of 1:500 is shown in Figure 1. The territory is located in the steppe zone. Esil settlement has coordinates  $51.1057^\circ$  North latitude and  $71.425^\circ$  East longitude.

Under the conditions of natural regime groundwater level is subject to seasonal fluctuations: the minimum standing is observed in March, the maximum falls on the beginning of May.

The amplitude of level fluctuation in the studied area amounted to 1.20-1.50 m.

At spring maximum it is necessary to expect groundwater level rise by 1.0 m, higher on the date of one-time groundwater level measurement on 23.09.2021.

The survey site is classified as potentially waterlogged.



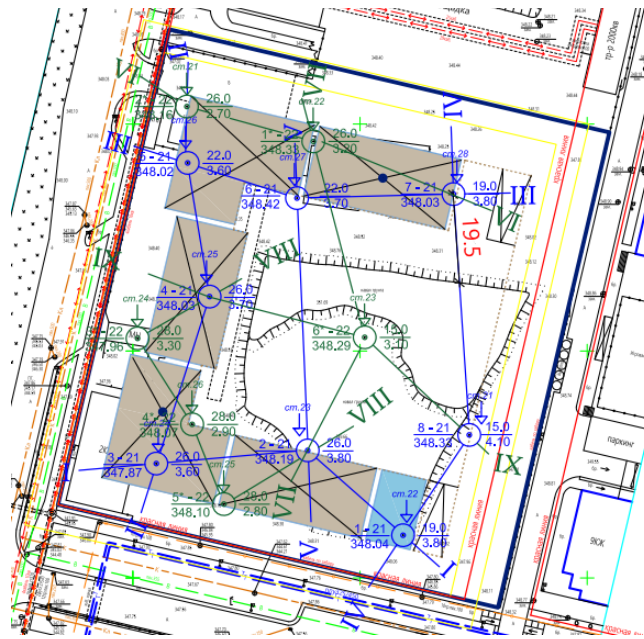


Figure 1 – Topographic survey of the object [11]

The topographic survey data shows that the spacing between boreholes exceeds 25 meters and the changes in absolute elevations range from 348.04 to 348.19 meters. As can be seen, the large distance between boreholes, which may complicate the accurate modeling of geologic structures and soil distribution at the site and require additional studies or survey methods to obtain a more complete picture of the geologic structure.

Based on the results of the analysis of physical and mechanical properties of soils by engineering-geological parameters, the following layers of soil occurrence are defined:

*Engineering-geologic element No. 1 (tQIV):* Bulk soil, dark brown in color, with hard consistency, containing construction debris and impurities of organic matter with a volume of 3.6%.

*Engineering-geologic element No. 2 (aQII-III):* A loam with a variable consistency ranging from firm to fluid-plastic, characterized by light brown and gray tints, with admixture of carbonates and interlayers of sand and loam up to 20 cm thick. The organic matter content varies from 3.20% to 5.70%, with an average value of 4.10%.

*Engineering-geologic element No. 3 (aQII-III):* Loam with hard and plastic consistency, light brown in color, with carbonate phenocrysts and sand interlayers up to 20 cm thick. The organic matter content varies from 2.30% to 3.50%, with an average value of 3.0%.

*Engineering-geologic element No. 4 (aQII-III):* Medium coarse sand, brown in color, saturated with water, with interlayers of loam up to 20 cm thick.

*Engineering-geologic element No. 5 (aQII-III):* Gravelly sand of brown color, saturated with water, with interlayers of loam up to 20 cm thick.

*Engineering-geologic element No. 6 (eCI):* Loam of various shades, ranging from maroon to greenish-yellow to dark red, with a firm to semi-hard consistency, containing up to 10 percent silt loam, as well as patches of ogeolensis and omanganeseization. There are interlayers of clay and sandy loam up to 20 cm thick.

*Engineering-geologic element No. 7 (eCI):* Woody loam of various shades, with hard and semi-hard consistency, containing patches of yellowing and omarganization, as well as interlayers of woody soil.

*Engineering-geologic element No. 8 (eCI):* Loamy sandy loam with various shades of gravel, with a hard consistency, containing patches of tin-ironing and omarganization.

The geologic data obtained show that the soil strata layering does not follow the order of geotechnical engineering elements (GEI). For example, in some boreholes, such as No. 5, it can be observed that the engineering geologic element No. 2 follows the engineering geologic element No. 5, while in other boreholes the soil layers are presented in the expected order.

In order to analyze the structure of the soil foundation, it is required to conduct additional research, process the obtained data, and adjust the design solutions taking into account the heterogeneity of the soil.

We used the method of kriging interpolation to determine the intermediate geotechnical properties of the soil, which allowed us to obtain predictions of the values of each property at each point of the studied area in the form of continuous maps. The results obtained were implemented in ArcGIS software using the kriging spatial variation method to accurately predict values in other areas. Thus, the kriging method provides us with useful and accurate predictions of intermediate geotechnical soil values based on available data. It is important to note that this method takes into account the characteristics of soil layering and transition between layers, which further improves the accuracy and reliability of the results obtained.

### 3. Results and Discussion

Based on the available data, which includes the results of soil samples from 8 wells, we use the Kriging interpolation method in ArcGIS to determine soil property values between these wells where the data are unknown. This method allows us to predict soil property values at all other points in the study area. We processed and loaded the soil mechanical property data into a map database and presented the results in Figures 3-5. Using this approach helps to reduce resource and time costs while providing reliable results of the study.

Figure 2 displays the distribution of different soil types in the study area using a variety of color ranges corresponding to soil types.

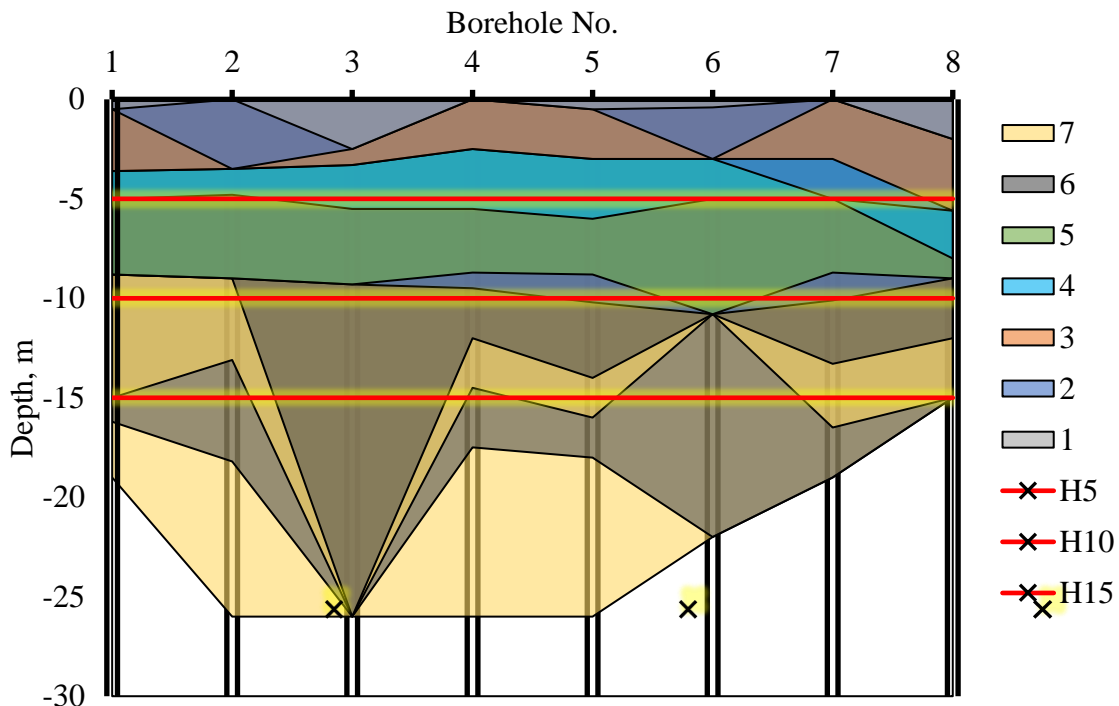


Figure 2 – Geological cross sections with

Figures 3-5 show the distribution of soil over the study area at different depths (5m, 10m, 15m), using a color scheme to visualize the results of the analysis of its mechanical properties ( $E_0$ ,  $c$ ,  $\phi$ ). In these schemes, the red color corresponds to the maximum values of the soil mechanical properties and the blue color corresponds to the minimum values. Areas with shades of gray and white show locations in the area where the values of soil mechanical properties are at an intermediate level, indicating their comparability with known data. Transparent areas on the map indicate minimal difference in the values of soil mechanical properties compared to known data.

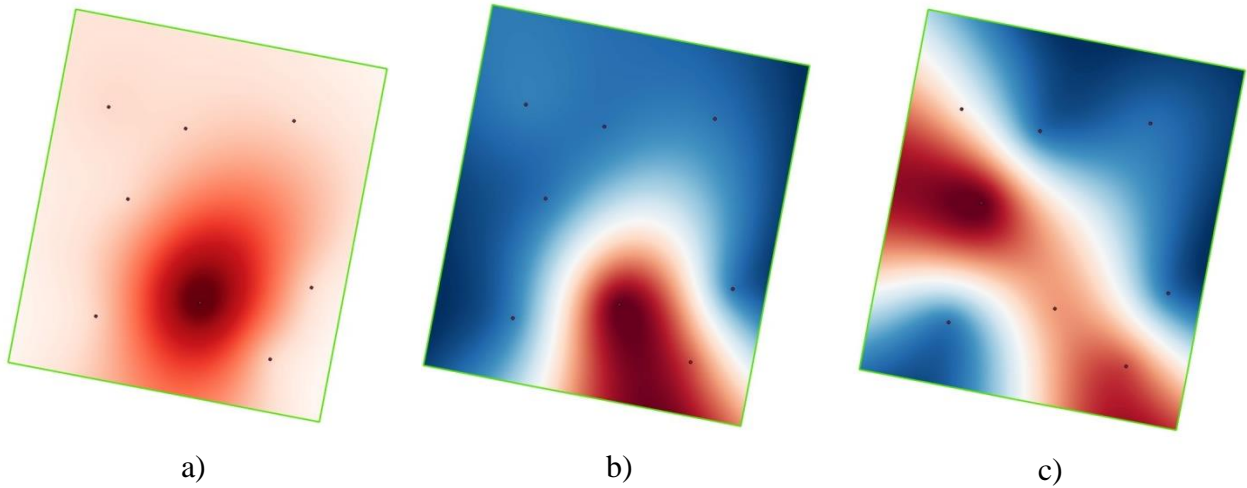


Figure 3 – Map of the study area showing the spatial variability of known values of total strain modulus “ $E_0$ ” at depths of a) 5 m; b) 10 m; c) 15 m

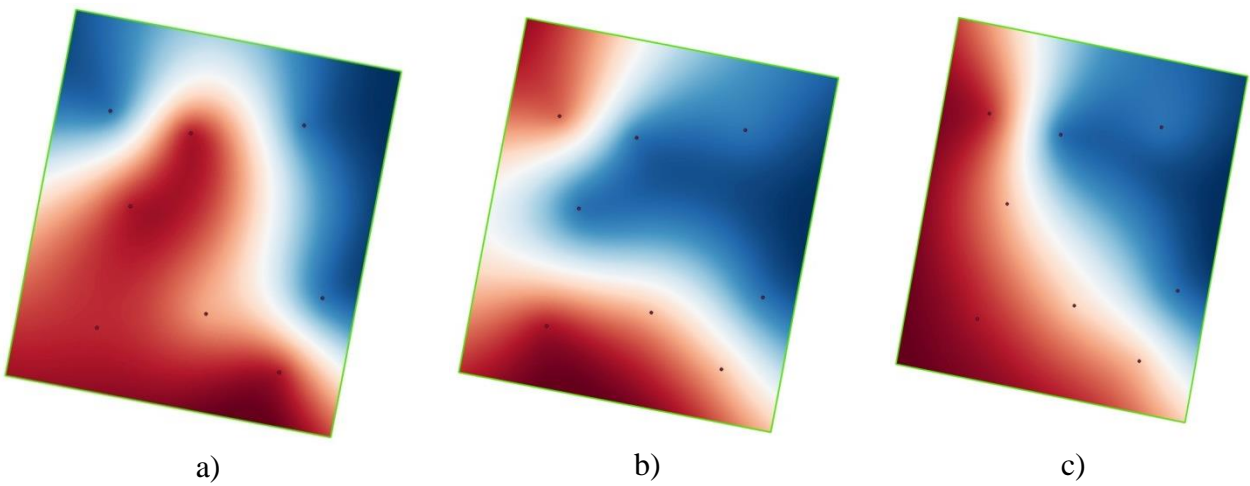


Figure 4 – Map of the study area showing the spatial variability of known specific gravity values “ $c$ ” at depths of a) 5 m; b) 10 m; c) 15 m

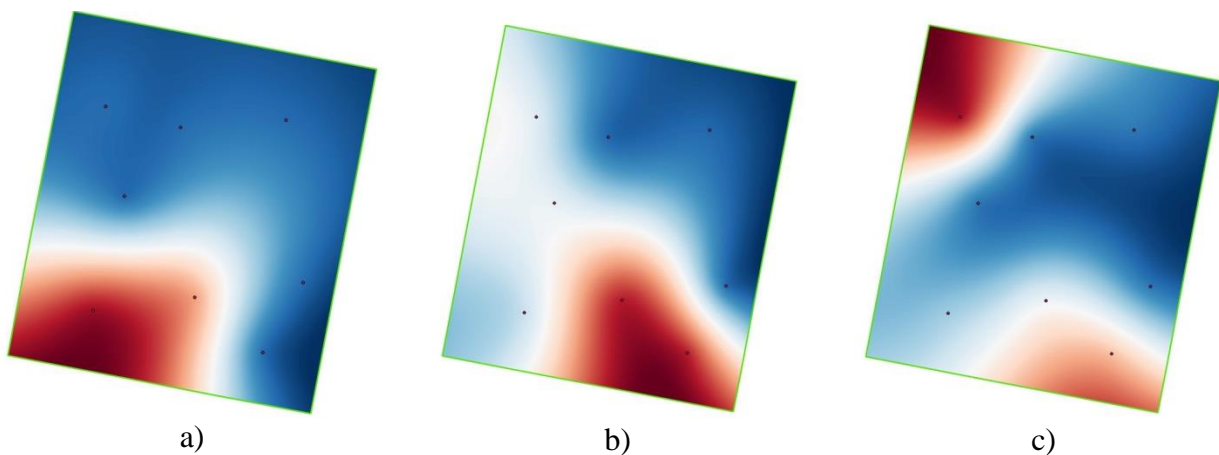


Figure 5 – Map of the study area showing the spatial variability of known values of internal friction angle “ $\varphi$ ” at depths of a) 5 m; b) 10 m; c) 15 m

By specifying the required depth and applying the recommended interpolation method, we can obtain intermediate geotechnical soil characteristics. This approach allows us to specify any depth and obtain accurate values of characteristics, which greatly facilitates the correct assessment

of engineering-geological conditions at the construction site. This, in turn, can lead to a reduction in the cost of survey work. In addition, using information on soil conditions from known boreholes, we can obtain data not only for idealized conditions, but also for realistic soil layering scenarios.

The proposed methodology serves as a practical tool for foundation footing visualization. It provides engineers with a comprehensive understanding of the mechanical characteristics of the soil, making it easier for designers to select optimal foundation types and sizes.

#### 4. Conclusions

To conclude the study on the application of geotechnical interpolation using GIS for foundation design, the following can be noted:

- the use of interpolation methods such as kriging in ArcGIS software can effectively determine the intermediate geotechnical properties of soils at the construction site, which allows engineers to obtain accurate values of soil characteristics at different depths, which facilitates the process of selecting optimal types and sizes of foundations;
- the kriging method provides accurate predictions of the values of geotechnical soil properties based on available data, which allows predicting the values of soil properties at all points in the study area, which facilitates more accurate planning and design;
- the use of GIS-assisted geotechnical interpolation is an important tool for visualizing foundation footings and provides engineers with a comprehensive understanding of soil mechanical properties, which not only improves the evaluation of geotechnical engineering conditions at the construction site, but can also lead to lower survey costs and optimize the foundation design process.

#### Acknowledgments

This study was funded by the Committee of Science of the Ministry of Science and Higher Education of the Republic of Kazakhstan (Grant No. AP19676116).

#### References

1. Geographic information systems and science: today and tomorrow / M.F. Goodchild // *Annals of GIS*. — 2009. — Vol. 15, No. 1. — P. 3–9. <https://doi.org/10.1080/19475680903250715>
2. Effects of inadequate geotechnical investigations on civil engineering projects / M. Zumrawi // *International Journal of Science and Research*. — 2014. — Vol. 3, No. 6. — P. 927–931.
3. Mapping Of Geotechnical Properties Using Arcgis: A Case Study of Abubakar Tafawa Balewa University Bauchi, Gubi Campus / I.I. Abdulkarim, H.U. Yahaya, D.D. Bagari // *Iconic research and engineering journals*. — 2022. — Vol. 5, No. 9. — P. 1–5.
4. Applications of GIS in Geotechnical Engineering: Some Case Studies / Amardeep Singh, Shahid Noor, R. Chitra, M. Gupta // *International Journal of Scientific Engineering and Science*. — 2018. — Vol. 2, No. 3. — P. 34–38.
5. Integrating GIS and spatial data analysis: problems and possibilities / M. Goodchild, R. Haining, S. Wise // *International journal of geographical information systems*. — 1992. — Vol. 6, No. 5. — P. 407–423. <https://doi.org/10.1080/02693799208901923>
6. GIS as a tool in geotechnical engineering / E.E. Hellawell, J. Lamont-Black, A.C. Kemp, S.J. Hughes // *Proceedings of the Institution of Civil Engineers - Geotechnical Engineering*. — 2001. — Vol. 149, No. 2. — P. 85–93. <https://doi.org/10.1680/geng.2001.149.2.85>
7. On the need for dependence characterization in random fields: Findings from cone penetration test (CPT) data / F. Wang, H. Li // *Canadian Geotechnical Journal*. — 2019. — Vol. 56, No. 5. — P. 710–719. <https://doi.org/10.1139/cgj-2018-0164>
8. A geographical information system managing geotechnical data for Athens (Greece) and its use for automated seismic microzonation / A.A. Antoniou, A.G. Papadimitriou, G. Tsiambaos // *Natural Hazards*. — 2008. — Vol. 47, No. 3. — P. 369–395. <https://doi.org/10.1007/s11069-008-9226-6>
9. A New Spatial Interpolation Approach Based on Inverse Distance Weighting: Case Study from Interpolating Soil Properties / J. Zhou, Z. Sha // *Geo-Informatics in Resource Management and Sustainable Ecosystem*: Vol. 399: Communications in Computer and Information Science. — Berlin, Heidelberg: Springer Berlin Heidelberg, 2013. — P. 623–631. [https://doi.org/10.1007/978-3-642-41908-9\\_61](https://doi.org/10.1007/978-3-642-41908-9_61)

10. GIS- Interpolated Geotechnical Zonation Maps in Surfers Paradise, Australia / H. Al-Ani, E. Oh, G. Chai, B. Nader Al-Uzairy // *GEOProcessing 2014: The Sixth International Conference on Advanced Geographic Information Systems, Applications, and Services*. — 2014. — P. 142–148.
11. Topographic survey, inv. No. 001224 dated 21.04.2021 / *Geo-Kaz Topography, LLP*. — 2021.

**Information about authors:**

*Aliya Aldungarova* – PhD, Associate Professor; 1) Project Supervisor, Solid Research Group, LLP, Astana, Kazakhstan; 2) Associate Professor, School of Architecture, Construction and Energy, D. Serikbayev East Kazakhstan Technical University, Ust-Kamenogorsk, Kazakhstan, [liya\\_1479@mail.ru](mailto:liya_1479@mail.ru)

*Assel Mukhamejanova* – PhD, Senior Lecturer, Department of Civil Engineering, L.N. Gumilyov Eurasian National University, Astana, Kazakhstan, [assel.84@list.ru](mailto:assel.84@list.ru)

*Nurgul Alibekova* – PhD, Associate Professor; 1) Senior Researcher, Solid Research Group, LLP, Astana, Kazakhstan; 2) Associate Professor, Department of Civil Engineering, L.N. Gumilyov Eurasian National University, Astana, Kazakhstan, [nt\\_alibekova@mail.ru](mailto:nt_alibekova@mail.ru)

*Sabit Karaulov* – Junior Researcher, Solid Research Group, LLP, Astana, Kazakhstan, [karaulovsabit1997@gmail.com](mailto:karaulovsabit1997@gmail.com)

*Daniyar Akhmetov* – Doctor of Technical Sciences, Associate Professor, Department of Construction and Building Materials, Satbayev University, Almaty, Kazakhstan, [d.a.akhmetov@satbayev.university](mailto:d.a.akhmetov@satbayev.university)

**Author Contributions:**

*Aliya Aldungarova* – concept, methodology.

*Assel Mukhamejanova* – analysis, visualization, editing.

*Nurgul Alibekova* – resources, data collection.

*Sabit Karaulov* – testing, modeling.

*Daniyar Akhmetov* – interpretation, drafting.

*Received: 20.03.2024*

*Revised: 21.03.2024*

*Accepted: 21.03.2024*

*Published: 21.03.2024*





## Calculation and numerical modeling of the effect of heat and mass transfer on the properties of pile foundations in seasonally freezing soils

Saltanat Mussakhanova<sup>1,\*</sup>, A.S. Sarsembayeva<sup>1</sup>, Askar Zhussupbekov<sup>1</sup>, Philip Collins<sup>2</sup>

<sup>1</sup>Department of Civil Engineering, L.N. Gumilyov Eurasian National University, Astana, Kazakhstan

<sup>2</sup>College of Engineering, Design & Physical Sciences, Brunel University, London, UK

\*Correspondence: [mussakhanova.saltanat@mail.ru](mailto:mussakhanova.saltanat@mail.ru)

**Abstract.** The phenomenon of heat and mass transfer in seasonally freezing soils has a significant impact on the condition of pile foundations. Building structures constructed in such soils experience extremely negative consequences: frost heave, vibration dynamics, moisture mass transfer and soil weakening during the thawing. Seasonally freezing soils occupy most of the territory of Kazakhstan, and in most regions the depth of soil freezing exceeds 1.5 m, there are settlements where the index reaches 1.97 m (Semiyaarka, East Kazakhstan region) and in the north of the country - 2.74 m (Arshaly, Akmola region). Arrangement of foundation bases below the frost depth leads to increased construction costs, requires additional costs for thermal insulation, ventilation, other materials and structures, and, in addition, does not always lead to a full levelling of the negative impact of heat and mass transfer on the term and conditions of operation of buildings, structures, railways and roads. Therefore, the efforts of engineers and specialists in the field of thermal physics are aimed at finding effective ways to solve the problems of deformation and destruction of foundations in seasonally freezing soils. In the article an attempt is made to reveal the character of heat and mass transfer influence on pile foundations in seasonally freezing soils on the basis of a thermomechanical model.

**Key words:** heat and mass transfer, pile foundations, seasonally freezing soils, frost heave deformations, thawing, freezing of soils.

### 1. Introduction

The relevance of the chosen topic of the study is due to the fact that seasonal freezing of soils is observed in the territory occupying more than half of the total area of Kazakhstan. Foundations in such soils are exposed to the influence of processes: freezing, frost heaving, thawing and vibrodynamics. These processes are especially intensive during seasonal thawing and freezing. The large extent of the territory of Kazakhstan from west to east and from north to south, the complexity of geographical, geological, tectonic, hydrogeological structure, landscape and climatic conditions have largely predetermined the peculiarity of seasonal freezing of soils in different regions of our country. Therefore, the main regularities of seasonal freezing at a particular site are determined by the conditions of heat exchange on the soil surface, its composition and condition. Figure 1 shows a schematic map of the maximum depth of penetration of the zero isotherm into the ground for Kazakhstan.

Pile foundations on seasonally freezing soils require a numerical study of the temperature regime, taking into account the processes of heat and mass transfer with phase transitions in order to determine their bearing capacity and stability to avoid further problems with the operation of buildings and structures [1].

The purpose of the article is to study the effect and patterns of heat and mass transfer on pile foundations in seasonally freezing soils.

The phenomenon of heat and mass transfer is actively investigated in thermophysics,

poromechanics and thermohydrodynamics. Migration processes occurring in thawing and freezing soils have been studied by: E.D. Ershov, A.I. Korotkiy, S. Krauch, O. Coussy, S.A. Kudryavtsev.

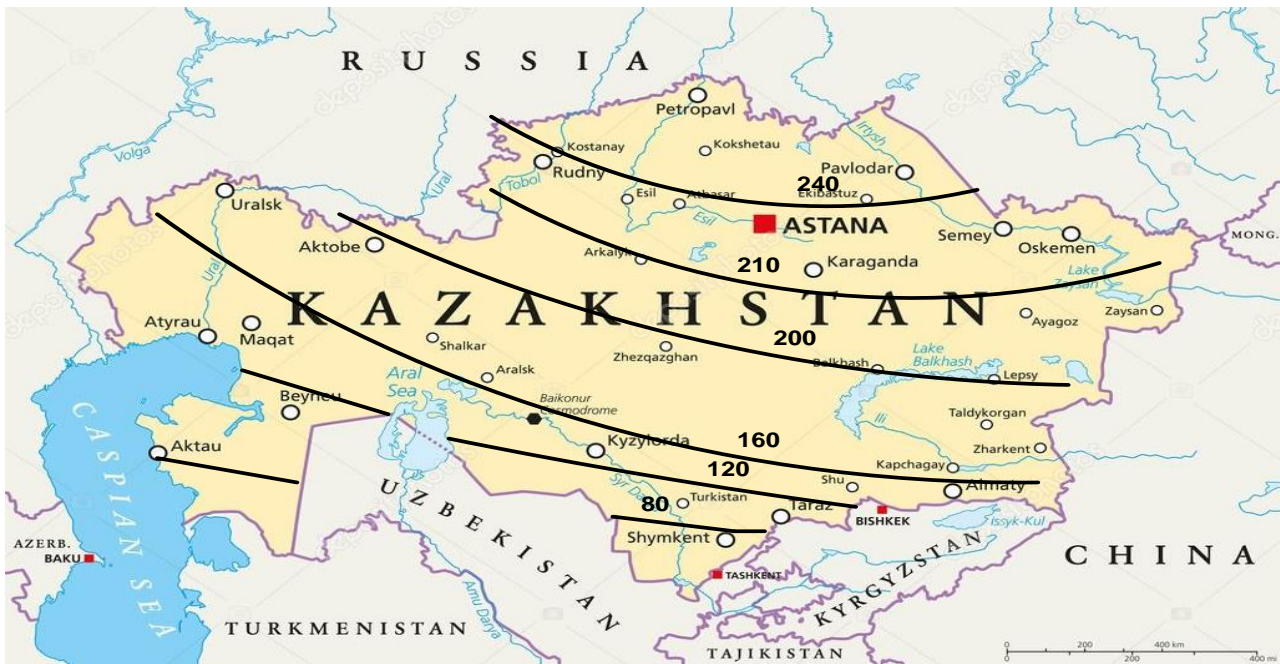


Figure 1 – Schematic map of the maximum depth of penetration of the zero isotherm into the ground [2]

Numerical and analytical methods for solving problems of heat and mass transfer in seasonally freezing soils are presented in the works of V.I. Popov, D.S. Skvortsov, E.M. Kartashov, A.Yu. Krainov, etc.

It should be noted that mathematical modelling of only the heat conduction process with phase transformation requires rather time-consuming iterative procedures. In the case of joint heat and mass transfer, the situation is aggravated and more than 150-300 iterations are required for joint solution of the mass and heat transfer equations in the known, at each time step, range of their variation. The reason for this is the incomplete use of those possibilities, which are determined by the phase equilibrium equation, linking the state parameters (temperature, moisture content, rock porosity, salt concentration in brine) satisfying the transport equations [3].

There are successfully tested numerical methods for approximate calculations of heat and mass transfer in soils (V.I. Popov, O.V. Tretyakova, etc.) [19]. In addition, today the solution of the heat and mass transfer problem by numerical and analytical methods is significantly facilitated by the use of special computer programmes, among which we can mention Frost Termo, Borey 3D, FrozenWall, Termoground. These programs allow to perform thermal and hydrodynamic calculations and provide opportunities for visual modelling of soil temperature fields and construction of necessary graphs and diagrams.

## 2. Methods

Laboratory methods of research were carried out, as a result of which we determined the soil filtration coefficient for Quaternary loams at the level of 0.01-0.13 m/day. Groundwater at this road section is characterised as sodium chloride, very hard, slightly alkaline, brackish. In relation to concrete of W4 grade on Portland cement, ground waters are non-aggressive and slightly aggressive, in relation to reinforced concrete structures they are moderately aggressive. Corrosive aggressiveness of ground water towards lead and aluminium cable sheathing is high. In relation to steel structures (according to Stabler) ground waters are corrosive. The main physical characteristics of the foundation soils are given in Table 1.

Table 1 – Results of laboratory analyses of foundation soils

Name of indicators	Unit	Value
Natural humidity	%	20.2
Liquid limit	%	26.5
Humidity at rolling limit	%	15.1
Plastisity index	%	11.6
Liquidity index		0.5
Soil density	g/cm <sup>3</sup>	2.00
Particle density of soil	g/cm <sup>3</sup>	2.70
Porosity coefficient	доли ед.	0.700
Moisture content	доли ед.	0.800
Deformation modulus	МПа	6.50
Specific cohesion	кПа	23.5
Angle of internal friction	degree	22

Partial values of strength and deformation properties of quaternary loams were subjected to static processing in accordance with the requirements of GOST 20522-2012 and as a result normative and calculated values of characteristics given in the table were obtained. The deformation modulus is 6.50 MPa. It is recommended to take the value equal to 6.0 MPa as the design value of the modulus of deformation.

The analysis of mechanical properties of foundation soils is given in Table 2.

Table 2 – Mechanical and deformation characteristics of foundation soils

Characteristics name	Unit	Values	on deformations $\alpha=0,85$	for load capacity $\alpha=0,95$
Specific cohesion	kPa	23.5	13.0	6.5
Angle of internal friction	degree	22	21	20
Deformation modulus	MPa	6.50	6.00	-
Soil density	g/cm <sup>3</sup>	2.00	1.98	1.97

To study the effect of heat and mass transfer on pile foundations in seasonally freezing soils, a thermohydrmechanical model of soil subjected to freezing and thawing processes was used.

This model assumes that the soil is a three-phase porous medium consisting of soil particles, liquid water and ice.

The thermohydrmechanical model includes a system of nonlinear equations consisting of mass transfer, heat transfer and equilibrium equations expressing such fundamental laws of continuum mechanics as the laws of conservation of mass, energy and momentum.

Important relations in the model are Bishop's formula for calculating the pore pressure in the freezing ground zone and the Clausius-Claiperon equation, which describes the intensity of cryogenic suction as a function of temperature [4].

The application of numerical modelling methods for the behaviour of pile foundations makes it possible to control by stages the processes of changes in temperature and moisture fields and associated deformations, and, consequently, to predict the efficiency of using various materials and measures to reduce or eliminate the negative phenomena acting on foundations and subgrade soils in conditions of their seasonal freezing-thawing [5].

We proceed from the assumption that seasonally freezing ground is a three-phase porous medium consisting of solid particles (index *s*), liquid water (index *l*) and ice crystals (index *i*).

In accordance with the existing ideas about the process of ground freezing, the following hypotheses are accepted for the construction of the thermohydrmechanical model:

- At the initial moment of time the porous medium is completely saturated with water;
- The rheological properties of porous medium under long-term loading are described by viscoelastic deformation [6].

### 2.1 Mass transfer equation

In accordance with the law of conservation of water and ice mass, the equation of mass

transfer taking into account the phase transition of pore water into ice can be written as Eq. (1):

$$\frac{\partial(\rho_j S_j n)}{\partial t} + \frac{\partial(\rho_i S_i n)}{\partial t} + \text{div}(\rho_l v_l) = 0 \quad (1)$$

Where:  $\rho S n$  – mass water content ( $j = l$ ) and ice ( $j = i$ ) at a point in time  $t$ ;  $\rho$  – phase density;  $S$ – phase saturation;  $n$ – porosity;  $v_l$ – water velocity relative to the solid skeleton.

Ice saturation  $S_i$  is given by a step function of temperature in Eq. (2):

$$S_i = \begin{cases} 1 - [1 - (T - T_{ph})]^\alpha, & T \leq T_{ph} \\ 0, & T > T_{ph}, \end{cases} \quad (2)$$

Where:  $T_{ph}$  – the freezing point of water;  $\alpha$  – experimental parameter.

Moisture saturation  $S_l$  is determined from the condition of complete saturation of the porous medium by the Eq. (3):

$$S_l = 1 - S_i. \quad (3)$$

The velocity of moisture movement  $v_l$  relative to soil particles is determined by Darcy's law by Eq. (4):

$$v_l = -k \cdot \text{grad}\psi, \quad (4)$$

Where:  $k$ – moisture conductivity coefficient;  $\psi$  – groundwater potential.

The moisture conductivity coefficient is calculated as a function of temperature in Eq. (5):

$$k = \begin{cases} k_0 [1 - (T - T_{ph})]^\beta, & T \leq T_{ph} \\ k_0, & T > T_{ph} \end{cases} \quad (5)$$

Where:  $k_0$  – moisture conductivity coefficient of unfrozen soil;  $\beta$  – experimental parameter [7].

Soil moisture potential is determined by the Eq. (6):

$$\psi = \frac{p_l}{\rho_l g} + z \quad (6)$$

Where:  $p_l$ – pore moisture pressure;  $g$  – free-fall acceleration;  $z$ – vertical coordinate.

Bishop's relationship is used to determine pore pressure by Eq. (7):

$$p = \chi p_l + (1 - \chi) p_i, \quad (7)$$

where  $p_i$  – ice pore pressure;  $\chi$  – coefficient depending on ice saturation.

The coefficient  $\chi$  is determined by the Eq. (8):

$$\chi = (1 - S_i)^{1.5}. \quad (8)$$

The ice pressure  $p_i$  is determined from the Clausius-Claiperon equation according to the expression in Eq. (9):

$$p_i = \frac{(\rho_l - \rho_i) p_0 + \rho_i \rho_l L \ln\left(\frac{T}{T_{ph}}\right) - \rho_i p_l}{\rho_l} \quad (9)$$

where  $L$ – specific heat of crystallisation of water;  $p_0$  – initial pore pressure.

From Eqs. (7) and (9) it follows that water pressure  $p_l$  can be calculated as a function of pore pressure  $p$  and temperature  $T$  by Eq. (10).

It follows from relations in Eqs. (7) and (9) that water pressure  $p_l$  can be calculated as a function of pore pressure and temperature using Eq. (10):

$$p_l = \frac{(1 - \chi)(\rho_l - \rho_i) p_0 + (1 - \chi) \rho_i \rho_l L \ln\left(\frac{T}{T_{ph}}\right) + \rho_l p}{\chi \rho_l + (1 - \chi) \rho_l} \quad (10)$$

## 2.2 Heat transfer equation

The heat transfer equation is derived from the law of conservation of energy, taking into account heat transfer due to the mechanisms of heat conduction and convection, as well as heat release during water crystallisation [8]. Then the heat transfer equation is written in the Eq. (11):

$$C \frac{\partial T}{\partial t} - \text{div}(\lambda \text{grad}T) + C_l v_l \cdot \text{grad}T = Q_{ph} \quad (11)$$

Where:  $C$  – volumetric heat capacity;  $\lambda$  – heat transfer coefficient of three-phase porous medium;  $C_l$  – volumetric heat capacity of water;  $Q_{ph}$  – heat source associated with the latent heat of the phase transition of water to ice.

The heat source  $Q_{ph}$  is determined by the Eq. (12):

$$Q_{ph} = L\rho_i \frac{\partial(nS_i)}{\partial t} \quad (12)$$

The volumetric heat capacity is calculated on the basis of the mixture rule according to the Eq. (13):

$$C = (1 - n)\rho_s c_s + n(S_l \rho_l c_l + S_i \rho_i c_i) \quad (13)$$

Where:  $c_j$  – is the specific heat capacity of the phase at constant pressure  $j(j = s, l, i)$ .

The heat transfer coefficient is calculated on the basis of the ratio for the stepped average as in Eq. (14):

$$\lambda = \lambda_s^{1-n} \lambda_l^{nS_l} \lambda_i^{nS_i} \quad (14)$$

Where:  $\lambda_j$  – phase heat transfer coefficient  $j(j = s, l, i)$ .

### 2.3 Equilibrium equation

It follows from the laws of poromechanics and momentum conservation that the equilibrium equation for a saturated porous medium can be written with respect to the total stress tensor  $\sigma$  in the Eq. (15)

$$\text{div}\sigma + \gamma = 0 \quad (15)$$

Where:  $\gamma$  – specific gravity of porous medium.

The specific gravity of the porous medium is determined by the Eq. (16):

$$\gamma = [(1 - n)\rho_s + n(S_l \rho_l + S_i \rho_u)]g \quad (16)$$

Where:  $\rho_s$  – soil particle density.

In turn, the total stress tensor can be through the effective stress  $\sigma$  tensor of the solid skeleton  $\sigma'$  and the pore pressure  $p$  by the Eq. (17)

$$\sigma = \sigma' - bpI \quad (17)$$

Where:  $I$  – unit tensor;  $b$  – effective Bio coefficient.

The effective stress tensor  $\sigma'$  is determined on the basis of Hooke's law for linear-elastic isotropic material from the relation in Eq. (18):

$$\sigma' = \left(K - \frac{2}{3}G\right) \varepsilon_{vol}^{el} I + 2G\varepsilon^{el} \quad (18)$$

Where:  $K$  – effective bulk modulus;  $G$  – effective shear modulus;  $\varepsilon^{el}$  – elastic strain tensor;  $\varepsilon_{vol}^{el}$  – volume elastic deformation value.

According to the principle of additive decomposition of the total strain tensor  $\varepsilon$ , the elastic strain tensor  $\varepsilon^{el}$  is defined by the Eq. (19):

$$\varepsilon^{el} = \varepsilon - \varepsilon^{th} - \varepsilon^{in} \quad (19)$$

Where:  $\varepsilon^{th}$  – temperature deformation tensor.

The total deformation tensor  $\varepsilon$  is defined from the geometrical relation for small deformations in the Eq. (20):

$$\varepsilon = \frac{1}{2}(\text{grad}(u) + \text{grad}(u)^T) \quad (20)$$

Where:  $u$  – displacement vector.

The temperature deformation tensor is defined by the Eq. (21):

$$\varepsilon^{th} = \alpha_T(T - T_0)I \quad (21)$$

Where:  $\alpha_T$  – thermal expansion coefficient;  $T_0$  – initial temperature of unfrozen ground.

The calculation of effective pore pressure is based on the equation of state by O. Coussy [9] as shown in Eq. (22):

$$p = N \left( n - n_0 - b\varepsilon_{vol}^{el} + 3\alpha_T(b - n_0)(T - T_0) \right) \quad (22)$$

Where:  $n_0$  – initial soil porosity;  $N$  – effective tangent modulus Bio.

The effective mechanical parameters are determined by the Eq. (23):



$$X = S_i X_{fr} + S_l X_{un} \quad (23)$$

Where:  $X$  – effective parameter value;  $X_{fr}$  и  $X_{un}$  – parameter values in frozen and unfrozen soil zones, respectively.

Keeping the divergent form of the equations, we obtain their Eq. (24):

$$\begin{cases} \frac{\partial(c\rho T)}{\partial t} = -\frac{\partial}{\partial x} J_Q + L_\rho I_F \\ \frac{\partial w}{\partial t} = -\frac{\partial}{\partial x} J_W - I_F \\ \frac{\partial(wC)}{\partial t} = -\frac{\partial}{\partial x} J_C - k_{3ax} C I_F - I_A \end{cases} \quad (24)$$

Where:  $I_A$  – ion adsorption index on the soil pore surface;  $I_F = -\partial m/\partial t$  – Moisture runoff due to water-ice phase transformations;  $k_{cap}$  – salt (ion) capture coefficient.

Flows are defined in accordance with the Eq. (25-27):

$$J_W = -K \frac{\partial w}{\partial x} + K \delta_{CW} \frac{\partial C}{\partial x} - K \delta_{TW} \frac{\partial T}{\partial x} J_Q + V_f = J_W^m + V_f \quad (25)$$

$$J_C = -W D_C \frac{\partial C}{\partial x} + C J_W = J_C^m + C V_f \quad (26)$$

$$J_Q = -\lambda \frac{\partial T}{\partial x} + c_W \rho_W T J_W = J_Q^m + c_W \rho_W T V_f \quad (27)$$

Where:  $\lambda$ ,  $K$ ,  $D_C$ ,  $c$ ,  $\rho$  – heat conductivity, moisture diffusion, salt diffusion, heat capacity and density coefficients, respectively;  $V_f$ – moisture filtration rate in porous material;  $\delta_{TW}$ ,  $\delta_{CW}$ – coefficients accounting for cross-effects [10].

The solution of the initial heat and mass transfer problem can be represented as a sequential solution of subproblems as follows:

- diffusion - system of Eq. (28):

$$\begin{cases} \frac{\partial(c\rho T)}{\partial t} = -\frac{\partial}{\partial x} J_Q^m \\ \frac{\partial w}{\partial t} = -\frac{\partial}{\partial x} J_W^m \\ \frac{\partial(wC)}{\partial t} = -\frac{\partial}{\partial x} J_C^m \end{cases} \quad (28)$$

– of the phase transition is the system of Eq. (29):

$$\begin{cases} \frac{\partial(c\rho T)}{\partial t} = L_\rho I_F \\ \frac{\partial w}{\partial t} = -I_F \\ \frac{\partial(wC)}{\partial t} = -k_{cap} C I_F \end{cases} \quad (29)$$

Solutions of the mass balance equations from Eq. (29) at each time step of Eq. (30):

$$w_2 = w_1 + \Delta m, \quad C_2 = C_1 + \left(\frac{w_1}{w_2}\right)^{1-k_{cap}} \quad (30)$$

The further course of action is shown in Figure 2.

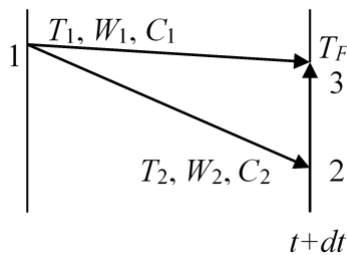


Figure 2 – Diagram of calculation of split heat and mass transfer processes

In Figure 2, transition (1-2),  $T_1 \rightarrow T_2$  is determined by the solution of system (28), transition (2-3),  $T_2 \rightarrow T_F$  is determined by the solution of system (29) [10].

### 3. Results and Discussion

On the example described in V.I. Vasiliev's thesis "Mathematical modelling of temperature regime of foundation soils in conditions of perennally frozen rocks thermo-hydro-dynamic model" the calculation of heat and mass transfer (Figure 3) in the system "pile - seasonally freezing ground" for the city of Astana was performed [17]:

- Soil parameters: for thawing zone  $\rho_j = 2,722 \cdot 10^6$ ,  $\lambda_j = 1,94$ ; for phase transition  $\rho_L = 125,532 \cdot 10^6$ ,  $\delta = 1.0$ ; for freezing zone  $\rho_i = 2,052 \cdot 10^6$ ,  $\lambda_i = 2,14$  [12];
- The geometrical area contains 20 piles (Figure 3); the pile dimensions are taken:  $r = 0.2$  m, length 14 m;
- Parameters were used as design parameters of the pile system:  $\nu T = 1.0$ ,  $\rho_p c_p = 1.763 \cdot 10^6$ ,  $R = 0.05$ ;
- Numerical modelling was carried out for the area with dimensions  $L_x = 15$  m,  $L_y = 54$  m,  $L_z = 50$  m;
- Numerical modelling was carried out for a region of size = 15 m, = 54 m, = 50 m;
- The Dirichlet boundary condition with a constant temperature of  $20^\circ\text{C}$  is given;
- Calculations were carried out for  $t_{max} = 2$  years, with step  $\tau = 1$  day;
- Initial ground temperature is assumed to be  $-4^\circ\text{C}$ ;
- Temperature at the upper boundary of the study area is set taking into account the amplitude of air fluctuation in Astana, which, according to SP RK 2.04-01-2017 varies from  $-51.6^\circ\text{C}$  (absolute minimum) to  $+41,6^\circ\text{C}$  (absolute maximum) [1].

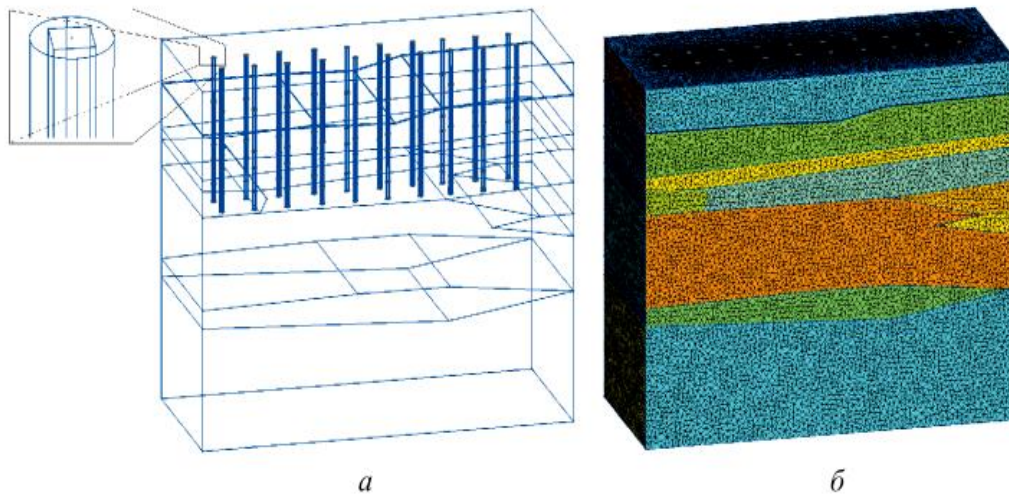


Figure 3 – Computational geometry (a) and tetrahedral mesh (b) for the heat transfer problem in soils taking into account the installation of 20 piles

It should be noted that in applied modeling, even when using significantly non-uniform computational meshes, the dimensionality of the heat transfer problem is quite large. For example, for our heat and mass transfer problem, the computational grid contains 260 thousand nodes, about 1.5 million tetrahedral cells. Numerical solution of such problems is impossible without the use of parallel architecture computing systems [11].

However, the algorithm we use is not associated with source averaging in spatial grid cells and can be generalised to multizone and multidimensional problems. The deviation of the calculation results from the exact solution of the test problem does not exceed 2-2.5%.

Figure 3 shows the results of calculations at a variable temperature of the medium. Inhomogeneous ice accumulation can be explained in different ways. V.I. Popov believes that "... periods of oscillation of the freezing front can be interpreted as its stopping near some average value" [12]. However, it follows from the works of E.D. Ershov [13], S. Crouch [14] and others that

the stopping of the front leads to moisture accumulation, as obtained in the present study.

Figure 4 shows the results of exposure of the ground to alternating temperatures with an initial temperature of  $-4\text{ }^{\circ}\text{C}$ . A characteristic feature of the result presented in Figure 4 is the slight spatial heterogeneity of ice accumulation. This is determined by the limited feeding area (melting zone) and low diffusion coefficient of moisture in the soil freezing zone.

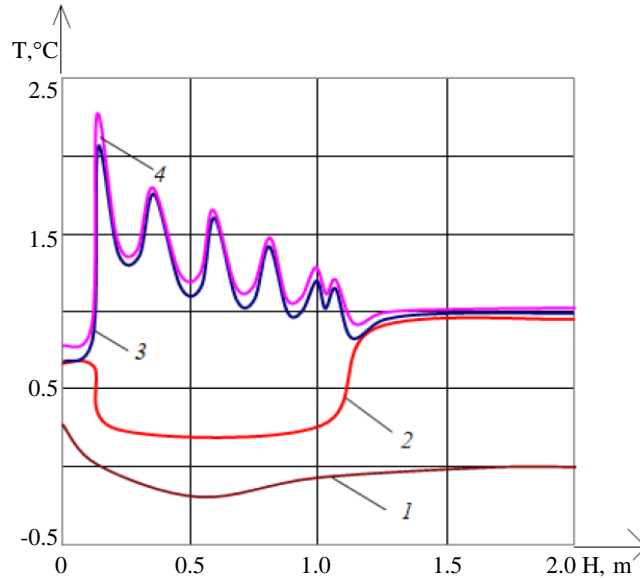


Figure 4 – Simulation results of temperature (1) -  $(T-273)/T_n$ , liquid phase (2) -  $w/w_0$ ; total moisture content (3) -  $(Lod + w)/w_0$  and concentration (4) -  $C/C_0$  fields

Figure 5 shows the distributions of temperature, moisture content and concentration fields during ground freezing under the influence of alternating temperature of the heat transfer medium for the case  $k_{cap} = 0.1$ .

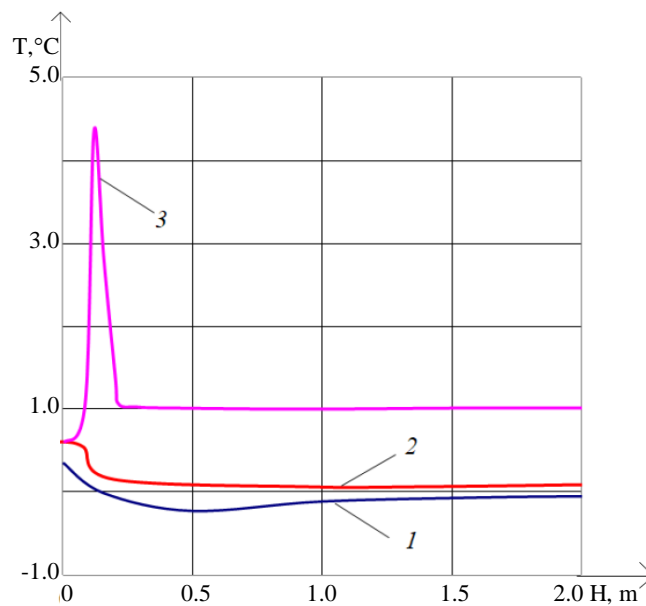


Figure 5 – Distribution of temperature (1), humidity (liquid phase) (2) and total humidity (3) fields [16]

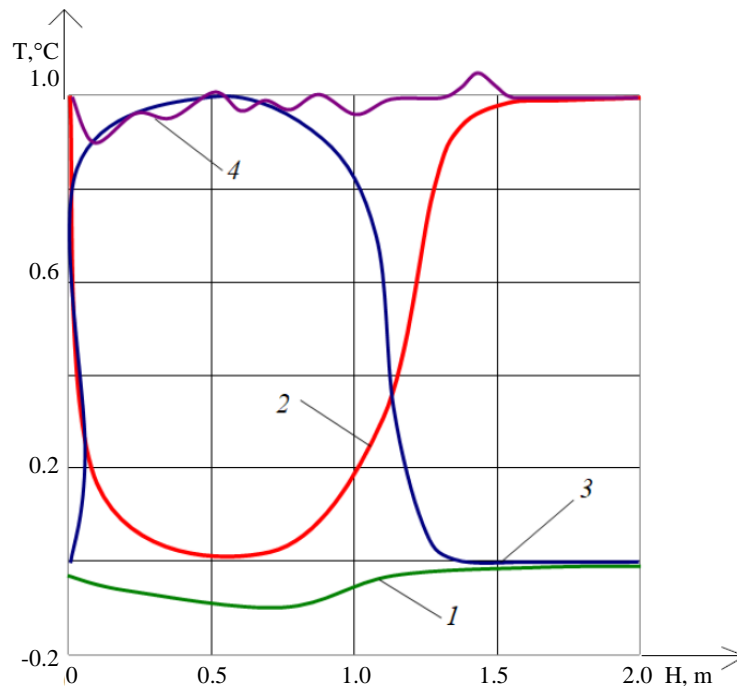


Figure 6 – Field distribution of temperature (1), moisture content (2) - liquid phase, (3) - solid phase - ice, concentration (4) [16]

Figure 6 shows that in the zone of active action of alternating temperatures (the rear front of ice formation) there is an inhomogeneous distribution of total concentration caused by alternating freezing and thawing of the ground. In addition, a significant inhomogeneity of the concentration distribution associated with displacement of the dissolved component is revealed at the front front of ice formation. This agrees with the data of numerical experiments conducted by Z.G. Ter-Martinosyan [15], V.I. Vasiliev (co-author) [16], I.I. Sakharov [17], and O.V. Tretyakova [18].

#### 4. Conclusions

According to the results of the study it is reasonable to formulate the further outcomes:

- A thermohydrodynamic model including a system of three nonlinear equations (mass transfer equation, heat transfer equation and equilibrium equation) has been applied to study the nature of the effect of heat and mass transfer on pile foundations in seasonally freezing soils;
- The mathematical model of heat, moisture and salt transport in dispersed composition during freezing-thawing of soil is formulated taking into account the functional relation between the parameters determining the phase equilibrium, mutual influence of diffusion flows and convective transport;
- The character of heat and mass transfer indicates an increase in ice accumulation, which leads to inhomogeneous vat of seasonally freezing soil; taking into account these features have an important practical significance for predicting the stability and reliability of pile foundations
- As a result of numerical modelling it was determined that the distribution of temperature fields at a depth of 0.8 m varies from 0 to 0.1 °c, the moisture content in the ground at temperatures up to 0 °c is in the liquid phase, at lowering it turns into the solid phase.

#### Acknowledgement

This work was funded by the Science Committee of the Ministry of Science and Higher Education of the Republic of Kazakhstan (Grant No. AP13268861).

#### References

1. Foundations on seasonally freezing soils / A.L. Nevzorov. — Moscow: ASV, 2022. — 152 p.

2. SP RK 2.04-01-2017 Building climatology. — 2017.
3. Teoriya teplomassoperenosa. Modelirovanie granichnyh zadach: uchebnoe posobie dlya vuzov / A.I. Korotkij, Yu.V. Starodubceva. — Moscow: Izdatelstvo Yurajt, 2024. — 168 p.
4. Numerical modeling of thermal stabilization of filter ground / P.N. Vabishchevich, M.V. Vasilyeva, N.V. Pavlova // Matematicheskoe modelirovanie. — 2014. — Vol. 26, No. 6. — P. 111–125.
5. SP RK 5.01-103-2013 Pile foundations. — 2013.
6. Sposoby borby s moroznym pucheniem sezonnopromerzayushih gruntov v osnovaniyah fundamentov zdaniy i sooruzhenij / D.S. Skvortsov, A.N. Kraev, A.N. Kraev, E.A. Zhaisambaev // The Eurasian Scientific Journal. — 2019. — Vol. 11, No. 5. — P. 1–12.
7. Teoriya teplomassoperenosa: reshenie zadach dlya mnogoslujnyh konstrukcij: uchebnoe posobie dlya vuzov / E.M. Kartashov, V.A. Kudinov, V.V. Kalashnikov. — Moscow: Izdatelstvo Yurajt, 2024. — 435 p.
8. Poromechanics / O. Coussy. — Chichester, UK: John Wiley & Sons, Ltd, 2003. — 298 p.
9. Chislennyye metody resheniya zadach teplo-i massoperenosa / A.Yu. Krainov, L.L. Minkov. — Tomsk: STT, 2023. — 92 p.
10. Geotekhnicheskoe modelirovanie processa promerzaniya i ottaivaniya morozoopasnyh gruntov / S.A. Kudryavtsev. — St. Petersburg: ASV, 2015. — 32 p.
11. SP RK 2.03-101-2012 Buildings and constructions in earned additionally territories and subsiding soil. — 2012.
12. Numerical solution of the problem of soil freezing / V.I. Popov, V.V. Popov // Mathematical modeling. — 2023. — Vol. 20, No. 5. — P. 121–130.
13. Deformacii i napryazheniya v promerzashih i ottaivayushih porodah / E.D. Ershov. — Moscow: MSU, 1985. — 167 p.
14. Metody granichnyh elementov v mehanike tverdogo tela / S. Crouch, A. Starfield. — Moscow: Mir, 1992. — 328 p.
15. Raschet kasatel'nogo napryazheniya moroznogo pucheniya vdol' stvola svai pri uchete yeye deformiruyemosti / Z.G. Ter-Martirosyan, P.A. Gorbachev // Zhilishchnoye stroitel'stvo. — 2022. — No. 12. — P. 36–39.
16. Mathematical Modeling of Temperature Regime of Soils of Foundation on Permafrost / V.I. Vasiliev, M.V. Vasilyeva, I.K. Sirditov, S.P. Stepanov, A.N. Tseev // Herald of the Bauman Moscow State Technical University. Series Natural Sciences. — 2017. — Vol. 70. — P. 142–159. <https://doi.org/10.18698/1812-3368-2017-1-142-159>
17. Reshenie trekhmernoj temperaturno-vlazhnostnoj zadachi promerzaniya i pucheniya na primere maloetazhnogo kirpichnogo zdaniya / I.I. Sakharov, V.N. Paramonov, K.G. Shashkin // Razvitie gorodov i geotekhnicheskoe stroitel'stvo. — 2011. — No. 2. — P. 1–12.
18. Normalnye napryazheniya moroznogo pucheniya kak funkciya izbytochnoj vlazhnosti / O.V. Tretyakova // Magazine of Civil Engineering. — 2017. — Vol. 76, No. 8. — P. 130–139.

### Information about authors:

*Saltanat Mussakhanova* – MSc, PhD Student, Department of Civil Engineering, L.N. Gumilyov Eurasian National University, 13 Kazhymukan st., Astana, Kazakhstan, [musaxanova.saltanat@mail.ru](mailto:musaxanova.saltanat@mail.ru)

*Assel Sarsembayeva* – PhD, Associate Professor, Department of Civil Engineering, L.N. Gumilyov Eurasian National University, 13 Kazhymukan st., Astana, Kazakhstan, [assel\\_enu@mail.ru](mailto:assel_enu@mail.ru)

*Askar Zhussupbekov* – Doctor of Technical Sciences, Professor, Department of Civil Engineering, L.N. Gumilyov Eurasian National University, 13 Kazhymukan st., Astana, Kazakhstan, [astana-geostroi@mail.ru](mailto:astana-geostroi@mail.ru)

*Philip Collins* – PhD, Deputy Dean, College of Engineering, Design & Physical Sciences, Brunel University London, London UB8 3PN, UK, [philip.collins@brunel.ac.uk](mailto:philip.collins@brunel.ac.uk)

### Author Contributions:

*Saltanat Mussakhanova* – concept, testing, data collection, funding acquisition.

*Assel Sarsembayeva* – editing, methodology, resources, interpretation.

*Askar Zhussupbekov* – analysis, drafting, editing.

*Philip Collins* – editing, analysis.

*Received: 20.03.2024*

*Revised: 21.03.2024*

*Accepted: 22.03.2024*

*Published: 22.03.2024*





## Comparative study of pile quality control techniques

 Abdulla Omarov<sup>1,\*</sup>,  Yoshinori Iwasaki<sup>2</sup>

<sup>1</sup>Department of Civil Engineering, L.N. Gumilyov Eurasian National University, Astana, Kazakhstan

<sup>2</sup>Geo-Research Institute, Co., Ltd., Osaka, Japan

\*Correspondence: [omarov\\_01@bk.ru](mailto:omarov_01@bk.ru)

**Abstract.** This article delves into the critical realm of quality control in pile foundation construction, presenting a comprehensive exploration of both destructive and non-destructive testing methodologies. Focused on enhancing structural integrity and reliability, the study evaluates techniques such as concrete strength testing, core sampling, Cross-Hole Sonic Logging (CSL), and Pile Integrity Testing (PIT). Results from field observations conducted during construction of the Light Rail Transit (LRT) system in Astana showcase the effectiveness of non-destructive methods, with 1,896 bored piles subjected to rapid testing. Significant findings reveal that approximately 75% of tested shafts exhibited anomalies, emphasizing the necessity for meticulous quality control. The article concludes by advocating for the adoption of advanced quality assurance protocols to mitigate risks and ensure the robustness of pile foundations in construction projects.

**Keywords:** pile foundations, quality control, non-destructive testing, structural integrity, reliability.

### 1. Introduction

Pile foundations constitute a vital aspect of construction projects, determining the structural integrity and longevity of buildings or structures [1]. Post-installation, a proportion of piles commonly exhibit defects stemming from manufacturing or transportation processes [2]. Various factors, such as inadequate concrete volume during concreting, interruptions in the concreting process, or compromised casing joints, can compromise the integrity of bored-injection piles [3]. Similarly, driven piles may incur defects due to safety breaches during transport or installation, subpar joint quality in composite piles, or concealed flaws in pile shaft fabrication. Consequently, factory defects in piles can render them unusable, leading to compromised integrity and reduced bearing capacity, affecting both soil and material. Such issues are prevalent across diverse pile construction methodologies, including bored, bored-injected, driven, or indentation piles. Despite the significance of pile quality control, it often receives cursory treatment, limited to maintaining records and concrete sampling at delivery [4]. However, such measures offer only indirect assessment, focusing on compliance with design specifications rather than manufacturing quality or shaft integrity. Consequently, there's a pressing need for a more robust quality control framework tailored to pile construction. Traditional testing methods, like static and dynamic load tests, while representative, only assess pile bearing capacity and fail to ensure reinforced concrete structure quality [5]. Direct quality control during drilling and concreting at construction sites often proves inadequate, lacking comprehensive operation-by-operation oversight. Hence, modern pile quality control techniques warrant investigation to address these shortcomings and enhance construction practices. This study aims to explore the effectiveness of contemporary pile quality control methodologies.

## 2. Methods

### 2.1 Destructive method of pile quality control

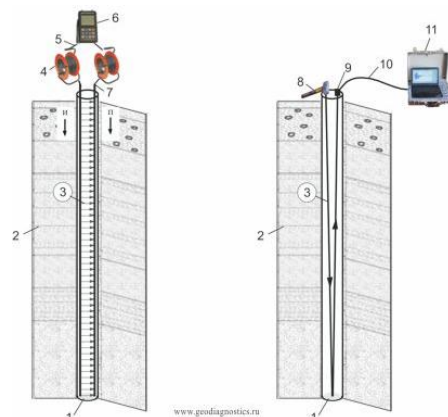
Concrete strength control for bored and driven piles follows [6], involving sampling from randomly selected mixes per [7], with at least two samples per batch and one per day. [8] guides sample preparation in verified moulds [9]. Testing yields an act indicating concrete strength. Samples should ideally cure in conditions mimicking structure hardening, but often cure externally, differing from borehole conditions. Hence, core samples drilled from pile shafts offer more representative results. Quality control includes strength testing of vertically drilled core samples at 0.5 m intervals. Sampling, overseen by the author, uses a small rotary drilling rig. Cores are labeled with details such as pile number, absolute mark, diameter, depth, and date. Quality control entails testing a minimum of two piles out of one hundred, increasing if defects are found. However, this method is destructive, labor-intensive, and costly, making comprehensive implementation impractical.

### 2.2 Non-destructive methods of pile quality control

Meanwhile, piles as responsible structures, the quality of which depends on the reliability of operation of the building (structure), must be subjected to continuous control. In contrast to destructive, the non-destructive methods are used for continuous control (Figure 1). Seismoacoustic (sound) and ultrasonic techniques are employed for assessing pile lengths, pinpointing defects like cracks and weakened sections, and evaluating the mechanical properties of pile concrete. Utilization of seismoacoustic and ultrasonic devices involves two main phases: conducting on-site pile tests and analyzing the acquired data with specialized software tools [10].



a) Destructive method



b) Non-destructive method



c) Cross-Hole-Analyzer (CHA)



d) Seismoacoustic and ultrasonic methods

Figure 1 – Pile quality control methods

### 2.3 Cross-Hole-Analyzer (CHA)

CHA uses a cross-hole acoustic survey method to determine the quality and consistency of concrete between pairs of PVC or steel pipes pre-installed in bored shafts, cast-in-place walls, bored piles, cast-in-place piles or other types of concrete foundations (Figure 2). The transmitter and receiver are in different conductive tubes, and it is important that they are at the same level when scanning. For these tests, the conductive holes are formed in advance using two steel or plastic tubes. Defects that are between the tubes are well defined, but since there is no radial scanning, there is a "dead zone" outside the tubes where defects cannot be detected. The main body of the pile can be examined using the required number of tubes (Figure 2).

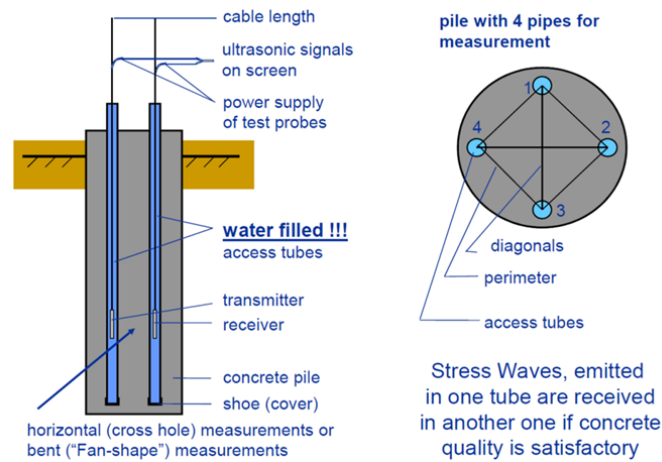


Figure 2 – Cross-Hole Sonic Logging principle

The number of conductive tubes increases significantly with the pile diameter (Figure 3).

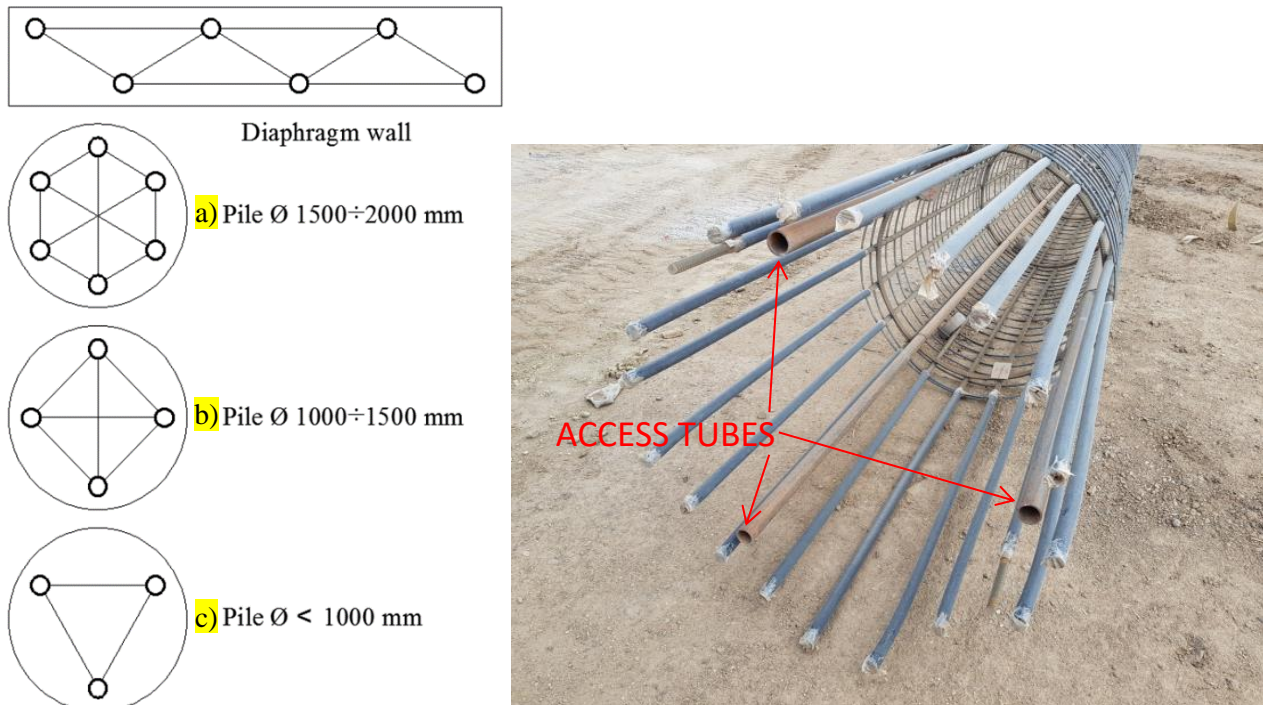


Figure 3 – Typical access tube configurations: a) scanning along three measurement directions; b) scanning along the perimeter and diagonals (six measurement directions).

The test cost correlates with the expense of constructing the conductive tubes. Discrepancies in concrete continuity or uniformity, typically on a decimeter scale, are identified through alterations in wave velocity or energy absorption, as illustrated in Figure 4.



## 2.4 Seismoacoustic method and ultrasonic method

Pile Integrity Tester (PIT). PIT performs integrity testing under small deformations according to also called acoustic echo testing. The PIT can be used for bored piles, bored shafts, driven piles, driven concrete pipes. It detects potentially dangerous defects such as significant cracks, neck formation, soil inclusions or cavities and, in some cases, can identify unknown dimensions of existing piles or test piles supporting existing bridges or abutments. Non-destructive quality control of pile continuity is based on the principle of acoustic flaw detection - the analysis of the passage and reflection in the structure (piles) under investigation of an acoustic wave, which is initiated by a calibrated impact on the pile head. The tests are carried out in accordance with ASTM D5882-16. The impact is produced by a special hammer with predetermined impact pulse parameters sufficient to dynamically excite the pile. The work also makes use of highly sensitive accelerometer sensors mounted on the pile head, as well as a separate analogue-digital instrument that includes a computer with a display and software that processes the information from the accelerometers. The resulting impact disturbance, modeled as a random uniaxial longitudinal compression wave, enters the pile body. A reflected wave is generated from the bottom of the pile and from defects in the pile, such as fractures, voids or cross-sectional inhomogeneity's, propagating in the opposite direction to the source of the original wave. To ensure the reception and registration of the secondary wave in piles, the removal (cutting down) of low-quality concrete is carried out beforehand, followed by leveling the surfaces of the pile caps for the installation of accelerometer sensors. The level of the surfaces of the pile caps after leveling should be horizontal. In order to increase the reliability of information on the results of pile testing, measurements are carried out at least at 3 different points of the pile caps. The measurement points (impact load applications) must be distributed evenly over the area of the caps. The accumulated signals are recorded in the computer memory for further processing and analysis. Figure 4 shows a graph of wave propagation in a rod with a weakened cross-section. An example of a narrowed cross-section of a bored pile. Processing, decoding and interpretation of low-frequency wave signals obtained during continuity testing of piles should be performed by a qualified specialist using special software.

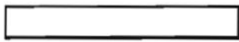





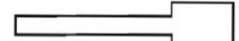



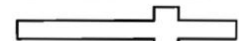


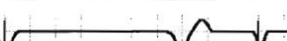
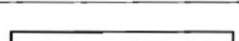





PILE PROFILE	DESCRIPTION	REFLECTOGRAM
	Straight pile	
	Straight pile	
	Straight pile	
	Increased	
	Decreased	
	Locally	
	Locally	
	High L/D ratio	
	Multipole reflections from	
	Irregular profile	

Figure 4 – Typical pile profiles with respective reflectograms

The pile continuity testing method relies on the principles of sound wave propagation, encompassing both high and low frequencies, within solid materials. It stands as one of the most contemporary techniques employed in global pile testing practices in recent years. This method facilitates comprehensive analysis of pile continuity across all pile types and enables the detection of structural defects within the pile body. Depending on the estimated velocity of plane wave propagation in concrete, this method allows for various determinations, including:

- 1) The approximate length of the piles;
- 2) Widening in the cross-section of the piles;
- 3) Narrowing in the cross-section of the piles;
- 4) Change in soil layers;
- 5) Change in pile material;
- 6) Transverse cracks in the pile shaft;
- 7) Inclusions of foreign material.

Various devices are used for ultrasonic pile testing: IDS-1 (Russia); Pocket Echo Tester and Pile Echo Tester (UK); Pile Integrity Tester-PIT (USA); and Sonic Integrity Tester-SIT (Netherlands).

Currently in Astana city works on construction of LRT (Light Rail Transit) public transport system are underway. Construction works are carried out by the Chinese company "China Railway Asia-Europe Construction Investment Co". Testing of bored piles by Pile Integrity Testing (PIT) and Cross-hole Sonic Logging (CSL) methods at the construction site of the object: "New transport system of Astana city. LRT", (section from the airport to the new railway station) was carried out with technical and financial support of L.N. Gumilev ENU and KGS LLP with the participation of the author. The tests were conducted at the LRT construction site in Astana. Nowadays non-destructive methods have become an effective technique to check the integrity of concrete deep foundations. The results of non-destructive tests carried out using rapid methods technology on bored piles located at 18 stations and interchanges were analysed. A total of 1,896 bored piles were tested between February and October 2018 [11]. During the production of bored piles, there is a risk of cavities and other defects. For example, soil particles may get into the concrete mix. To detect defects, the integrity of the bored pile is examined (Figure 5).



Figure 5 – CSL pile testing with two probes

### 3 Results and Discussion

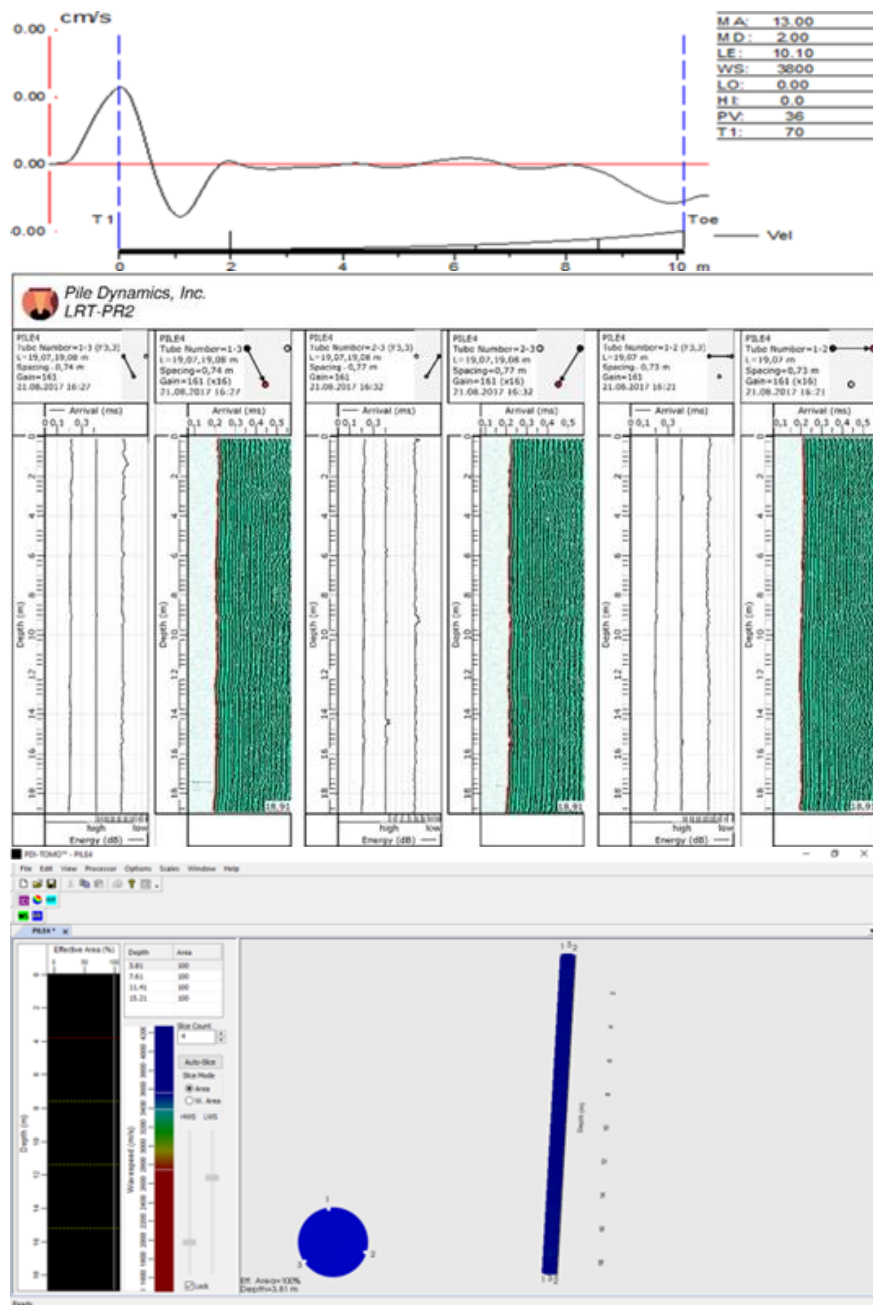
Reinforced concrete piles are frequently utilized as a substitute for deep foundations, especially in challenging soil conditions or where vibration from pile driving is unsuitable. Despite



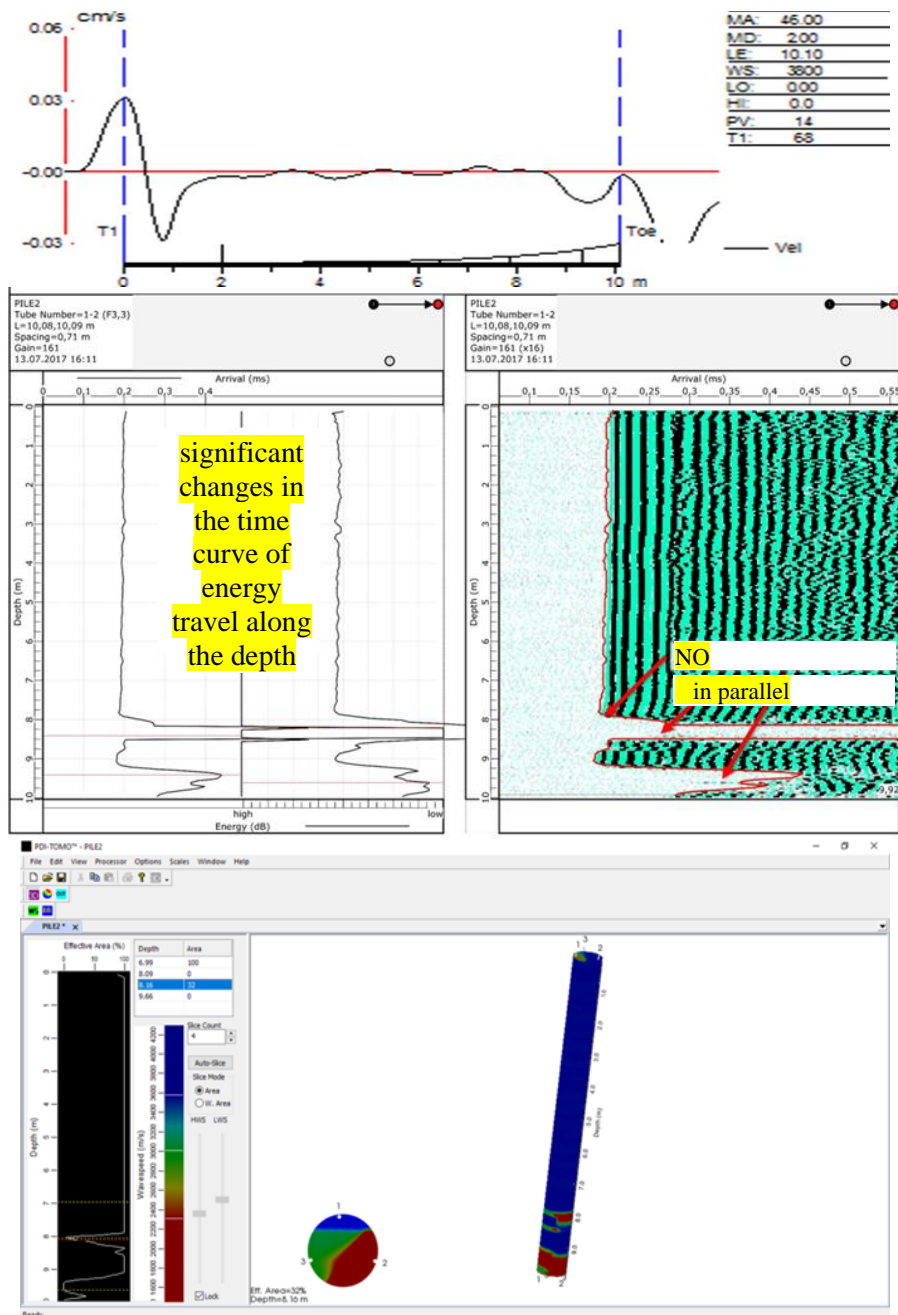
the implementation of quality control measures during initial foundation installation, validating the integrity of drilled shafts during construction, particularly in damp conditions, remains challenging. [12] observed that in over 400 drilled shafts tested across multiple projects in South Carolina, roughly 75% exhibited anomalies, with more than 30% of all shafts containing at least one anomaly. Bored shafts typically bear higher design loads than driven piles, resulting in lower repeatability, as highlighted by the findings of [13]. Given the elevated likelihood of anomalies in drilled shafts and their diminished repeatability, ensuring the quality of each drilled shaft holds paramount importance for every pile [14-15].

There is a set of rules according to which the quality control of bored pile production is determined. The CSL method of pile integrity inspection is considered to be the most effective. The physics of the process is that the speed of propagation of the sound wave changes depending on the structure of the material and its physical and mechanical properties.

The signal is recorded and compared to a reference signal. The difference in the signals characterizes the condition of the material in the piles (see Figure 6).



a) Results of "good" piles



b) Results of "bad" piles

Figure 6 – The tests were carried out at the LRT construction site in Astana

Low Strain Testing constraints:

- Detectable: Pile length, inclusions of foreign material with different acoustic properties, cracking perpendicular to the axis, joints and staged concreting, abrupt changes in cross section, distinct changes in soil layers.

- Undetectable by Sonic Test: The toe reflection when the Length/Diameter ratio roughly exceeds 20, gradual changes in cross-section, minor inclusions and changes in cross-section, impedance changes of small axial dimension, small variations in length, features located below either a fully-cracked cross section, debris at the toe, deviations from the straight line and from the vertical, the consistency of concrete cover, the length of reinforcement.

Cross-Hole Sonic Testing constraints:

- Detectable: Multiple defects, "soft bottoms" if tubes go to the bottom, voids better than soil inclusions, larger defects easier than small defects, waterfall, FAT (First Arrival Time), and energy all help find defects.

- Undetectable by Cross-Hole Sonic Test: Diameter changes or bulges, if too few tubes, can miss a defect, can find defect on direct path, cannot find defect outside cage, major diagonal defects more difficult to find, need more than 4 tubes for 1500 mm pile (recommend 6 tubes for shaft this size).

#### 4 Conclusions

1. Effective interpretation of PIT test results hinges on both the expertise of the test operator and the meticulous calibration of the instruments.

2. The cost-effectiveness of implementing a quality control program at each construction site far outweighs the potential losses stemming from undetected foundation defects.

3. While the Low Strain test is a cost-effective and efficient quality-control tool, it is essential to recognize its limitations. Despite its quick application time and affordability, it is not infallible. Additionally, the sonic method's efficacy relies on identifying pile attributes that significantly impact wave propagation, typically those of substantial size.

4. Cross-hole logging testing stands out as the most accurate and high-quality method for field observation of deep pile foundations.

#### Acknowledgments

This research was funded by the Science Committee of the Ministry of Science and Higher Education of the Republic of Kazakhstan. (Grant No. AP13268718).

#### References

1. Structural Stability: A Comprehensive Review of Pile Foundations in Construction / F. Kaladi, F. Wang, F.Z. Kherazi // Journal of Asian Development Studies. — 2023. — Vol. 12, No. 4. — P. 412–425.
2. Introduction to Pile Driving Inspection / K. Beard // Employee Training Manual. — Louisiana: LTRC, 2011.
3. Integrity Problems of Concrete Piles / FPrimeC. — 2017.
4. Non-destructive testing of bored piles / A. Tulebekova, N. Shakirova, A. Zhankina, Y. Muratov // Technobius. — 2021. — Vol. 1, No. 3. — P. 0002. <https://doi.org/10.54355/tbus/1.3.2021.0002>
5. Assessment of the bearing capacity of piles in soil, determined by static and dynamic load tests / R.E. Lukpanov, S.B. Yenkebayev, D.V. Tsigulyov // Engineering Journal of Satbayev University. — 2021. — Vol. 143, No. 2. — P. 252–260. <https://doi.org/10.51301/vest.su.2021.i2.33>
6. GOST 18105-2018 Concretes. Rules for control and assessment of strength. — 2018.
7. GOST 10181-2000 Concrete mixtures. Methods of testing. — 2000.
8. GOST 10180-2012 Concretes. Methods for strength determination using reference specimens. — 2012.
9. GOST 22685-89 Moulds for making control specimens of concrete. Specifications. — 1989.
10. The Experience of Piling Tests on Astana LRT Construction Site / A.Zh. Zhussupbekov, A.R. Omarov, N. Shakirova, B.G. Abdrakhmanova, D. Razueva // Proceedings of the 16th Asian Regional Conference on Soil Mechanics and Geotechnical Engineering, ARC 2019. — Taipei, Taiwan: 2020. — P. TC305.
11. Complex Analysis of Bored Piles on LRT Construction Site in Astana / A. Zhussupbekov, A. Omarov, N. Shakirova, D. Razueva // Transportation Soil Engineering in Cold Regions, Volume 1: Vol. 49: Lecture Notes in Civil Engineering. — Singapore: Springer Singapore, 2020. — P. 461–471. [https://doi.org/10.1007/978-981-15-0450-1\\_48](https://doi.org/10.1007/978-981-15-0450-1_48)
12. Crosshole Sonic Logging of South Carolina Drilled Shafts: A Five Year Summary / W.M. Camp, Iii, D.W. Holley, G.J. Canivan // Contemporary Issues In Deep Foundations. — Denver, Colorado, United States: American Society of Civil Engineers, 2007. — P. 1–11. [https://doi.org/10.1061/40902\(221\)2](https://doi.org/10.1061/40902(221)2)
13. Defect Analysis for CSL Testing / G. Likins, F. Rausche, K. Webster, A. Klesney // Contemporary Issues In Deep Foundations. — Denver, Colorado, United States: American Society of Civil Engineers, 2007. — P. 1–10. [https://doi.org/10.1061/40902\(221\)3](https://doi.org/10.1061/40902(221)3)
14. Non-Destructive Testing of Piles Using the Low Strain Integrity Method / N. Massoudi, W. Teferra // Proceedings of the International Conference on Case Histories in Geotechnical Engineering: Vol. 2. — Missouri: 2004. — P. 1–6.
15. Low Strain Testing of Piles Utilizing Two Acceleration Signals / M. Johnson, F. Rausche // Proceedings of the Fifth International Conference on the Application of Stress-wave Theory to Piles. — Orlando, Florida: 1996. — P. 859–869.

**Information about authors:**

*Abdulla Omarov* – PhD, Senior Lecturer, Department of Civil Engineering, L.N. Gumilyov Eurasian National University, Astana, Kazakhstan, [omarov\\_01@bk.ru](mailto:omarov_01@bk.ru)

*Yoshinori Iwasaki* – PhD, Professor, Geo-Research Institute, Co., Ltd., Osaka, Japan, [dec19yoshi1+torino@gmail.com](mailto:dec19yoshi1+torino@gmail.com)

**Author Contributions:**

*Abdulla Omarov* – concept, methodology, resources, data collection, testing, modeling, analysis, funding acquisition.

*Yoshinori Iwasaki* – visualization, interpretation, drafting, editing.

*Received: 20.03.2024*

*Revised: 25.03.2024*

*Accepted: 25.03.2024*

*Published: 25.03.2024*